Leptin antagonism improves Rett syndrome phenotype in symptomatic male *Mecp2-null* mice.

Yasmine Belaïdouni[1], Diabe Diabira[1], Mélanie Brosset-Heckel[1], Victoria Valsamides[1], Jean-Charles Graziano[1#], Catarina Santos[3], Clément Menuet[1], Gary A. Wayman[2] and Jean-Luc Gaiarsa[1*].

[1]INMED, INSERM, Aix Marseille Univ, France.

[2]Program in Neuroscience, Department of Integrative Physiology and Neuroscience, Washington State University, Pullman, WA, United States.

[3]Phenotype Expertise, Marseille, France.

[*]Correspondence to: jean-luc.gaiarsa@inserm.fr

#present address: Aix-Marseille Univ, Institut Paoli Calmettes, INSERM, CNRS, CRCM, Marseille, France.

Running head: Rett syndrome and leptin.

Key words: leptin, breathing, Rett syndrome, hippocampus, E/I balance, Mecp2.

ABSTRACT

Rett syndrome (RTT) is a severe neurodevelopmental disorder that arise from *de novo* mutations in the X-linked gene *MECP2* (methyl-CpG-binding protein 2). Circulating levels of the adipocyte hormone leptin are elevated in RTT patients and rodent models of the disease. Leptin targets a large number of brain structures and regulates a wide range of developmental and physiological functions which are altered in RTT. We hypothesized that elevated leptin levels might contribute to RTT pathogenesis. Accordingly, we show that pharmacological antagonism of leptin or genetic reduction of leptin production prevents the degradation of health status, weight loss and the progression of breathing and locomotor deficits. At the neuronal level, the anti-leptin strategies rescue the hippocampal excitatory/inhibitory imbalance and synaptic plasticity impairment. Targeting leptin might therefore represent a new approach for RTT treatment.

INTRODUCTION

Rett syndrome (RTT; OMIM identifier #312750) is a rare non-inherited genetic neurodevelopmental disorder characterized by severe impairments affecting nearly every aspect of child‘s life. After an apparently normal development until about 6–18 months of age, RTT patients undergo a period of rapid regression including, but not limited to, loss of purposeful hand movements, loss of acquired speech, breathing irregularities, seizures, and severe cognitive deficits (Sandweiss et al., 2020). Typical RTT cases arise from *de novo* mutations in the X-linked gene *MECP2* (methyl-CpG-binding protein 2). The MECP2 protein binds to methylated DNA to modulate the expression of thousands of genes (Lewis et al., 1992) and plays an important role in brain development and functioning throughout the lifespan (Cheval et al., 2012) .

Several clinical features of the human disorder are recapitulated in *Mecp2*-deficient mice (Ricceri et al., 2008). These mouse models therefore represent an essential tool for deciphering the cellular mechanisms of the disease and for testing potential therapeutic treatments. The demonstration that phenotypic rescue is possible in *Mecp2*-deficient mice upon re-expressing *Mecp2* gene in adult mice (Guy et al., 2007) has indicated that RTT is not an irrevocable disease, giving hope for therapeutic interventions.

Many aspects of neurochemistry are altered in RTT, including the levels of neurotrophic factors and neuromodulators, some of which holding therapeutic promises (Ehinger et al., 2018). Among these deregulated factors, epidemiological and animals studies showed that the circulating levels of leptin are elevated in RTT patients and rodent models of the disease (Blardi et al., 2007, 2009; Acampa et al., 2008; Park et al., 2014; Fukuhara et al., 2019). Leptin, the product of the obese (*ob*) gene, is a circulating hormone secreted mainly from the white adipocytes and transported across the blood brain barrier to the hypothalamus, to suppress food intake (Ahima and Flier, 2000). It is increasingly clear that the hypothalamus is not the only site of leptin action, and that food intake is not its only biological role. Leptin is a pleiotropic hormone that modulates motivation (Davis et al., 2010), cognitive functions (Harvey, 2022), anxiety (Guo et al., 2012), the excitability of neuronal networks (Shanley et al., 2002), epileptiform activities (Mora-Muñoz et al., 2018), breathing activity (Gauda et al., 2020), and more (Signore et al., 2008; Lim et al., 2009; Li et al., 2018). Large bodies of evidence also indicate that leptin acts as an important neurotrophic factor during perinatal periods promoting neuritic growth and synaptogenesis in a variety of brain structures including the hypothalamus (Bouret et al., 2004; Pinto et al., 2004) and hippocampus (O'Malley et al., 2007; Moult and Harvey, 2008; Dhar et al., 2014; Dumon et al., 2018; Sahin et al., 2020, 2021). Due to these

important physiological and developmental functions, dysregulation – either excess or deficiency – in leptin availability or signaling can have far reaching effects. Accordingly, animal studies showed that abnormal leptin levels at any time of lifespan can lead to adverse outcomes including social and cognitive impairments, altered breathing activity, seizures susceptibility and abnormal brain development (Harvey, 2003; Greco et al., 2010; Dumon et al., 2018; Mora-Muñoz et al., 2018; Gauda et al., 2020). Thus, excess levels of leptin in RTT patients (Blardi et al., 2007, 2009; Acampa et al., 2008) might contribute to the disorders associated with Rett syndrome.

To address this hypothesis, we confirmed an excess of serum leptin in male *Mecp*$^{2tm1\text{-}1Bird}$ mice (hereafter referred to as *Mecp2*$^{-/y}$ mice) and assessed the effects of "anti-leptin" strategies in ameliorating deficits typically displayed by this RTT mouse model. We show that pharmacological antagonism of leptin or genetic reduction of leptin production prevents the degradation of health status, weight loss as well as the progression of breathing and locomotor deficits in male *Mecp2*$^{-/y}$ mice and, at the neuronal level, rescues the hippocampal excitatory/inhibitory imbalance and synaptic plasticity impairment.

RESULTS

Serum leptin levels and leptin mRNA expressions are altered in *Mecp2*$^{-/y}$ mice.

The aim of this study was to assess the contribution of leptin in RTT. Therefore, as a prerequisite for this study, we evaluated the circulating levels of leptin by ELISA, and the *Lep* mRNA expression from two main sources of leptin, the white adipose tissues (WAT) and gastrocnemius muscle, by qRT-PCR in male *Mecp2*$^{-/y}$ and WT littermates. We found that *Mecp2*$^{-/y}$ mice exhibited elevated circulating leptin levels compared to WT littermates, and that this difference reach significance at postnatal day (P) 30 and 50 ($p=0.045$ and 0.0002 respectively, Two-tailed unpaired *t*-test, **Figure 1A, supplementary table 1**). Interestingly, the elevated level of leptin in *Mecp2*$^{-/y}$ mice was observed despite their decrease in body weight (19.8 ± 0.6 vs 13.6 ± 0.5g, $p<0.0001$, two-tailed unpaired *t*-test, **Figures 1B**). *Mecp2*$^{-/y}$ mice also exhibited higher expression of leptin mRNA in gastrocnemius muscle (**Figure 1C**), as well as in visceral and inguinal WAT (**Figures 1D and E**) compared to their WT littermates. The difference reaches significance at P30 in inguinal WAT ($p=0.03$, Two-tailed unpaired *t*-test, **supplementary table 1)** and at P50 in gastrocnemius muscle ($p=0.0015$), visceral WAT ($p=0.03$) and inguinal WAT ($p=0.03$, Two-tailed unpaired *t*-test, **supplementary table 1**). Altogether, these data show that circulating leptin levels and leptin mRNA expression are elevated in male *Mecp2*$^{-/y}$ mice compared to their age-matched WT littermates, providing a framework to assess the role of leptin in RTT-associated symptoms.

Leptin antagonism during the symptomatic stage prevents the progression of breathing deficits in *Mecp2*$^{-/y}$ mice.

Respiratory disorders have been well described in patients and rodent models of RTT (Ramirez et al., 2013). Leptin has been reported to regulate breathing acting on brainstem respiratory networks and carotid body (Gauda et al., 2020). We therefore investigate the possible contribution of leptin to RTT-associated breathing disorders. We first characterized the respiratory activity of *Mecp2*$^{-/y}$ mice from our breeding colony. Consistent with previous studies (Katz et al., 2009), when compared with their age-matched WT littermates, P40 *Mecp2*$^{-/y}$ mice developed respiratory disorders characterized by increased number of apneas ($p<0.0001$, Two-tailed unpaired *t*-test, **Figure 2A, supplementary table 2)**, cycle duration variability expressed as breathing irregularity score (14.6±0.7 vs 21.5±0.8, 28 and 29 mice, $p<0.0001$, Two-tailed unpaired *t*-test, **data not shown**), and minute ventilation (5.5±0.4 vs 9.4±0,7 ml g^{-1} min^{-1}, 28 and 29 mice, $p<0.0001$, Two-tailed unpaired *t*-test, **data not shown**). These breathing distresses worsen with age in *Mecp2*$^{-/y}$ mice, while the respiratory parameters remained constant in WT (**Figures 2B and C, supplementary table 2**). Next, to test the possible role of leptin in RTT-associated breathing disorders, P40 WT and *Mecp2*$^{-/y}$ mice received daily sub-cutaneous injection of leptin recombinant (5µg/g) or every other day sub-cutaneous injection of a pegylated leptin antagonist (5µg/g) (Gertler and Elinav, 2014), during 10 days. Sham mice received the same volume of vehicle. We used plethysmography to record breathing activity of each mouse at P40, the day before the start of treatment, and at P50, the last day of treatment. Leptin treatment of WT mice led to a significant increase in the number of apneas ($p=0.017$ when compared to P40, Two-tailed paired *t*-test, **Figure 2B,** $p=0.012$ when compared to P50 sham WT mice, Two-tailed unpaired *t*-test, **Figure 2D, supplementary table 2**) and breathing irregularity score ($p=0.04$ when compared to P50 sham WT mice, Two-tailed unpaired *t*-test**, Figures 2E, supplementary table 2**), while in sham WT mice these parameters remained unchanged (**Figures 2B, D and E, supplementary table 2**). The mean values of tidal volume (**data not shown**), respiratory

frequency (**data not shown**) and minute ventilation (p=0.72 when compared to P50 treated WT mice, Two-tailed unpaired *t*-test, **Figure 2F, supplementary table 2**) were not affected by the leptin-treatment.

We next investigated the effect of anti-leptin treatment (5µg/g, every other day during 10 days) on the breathing activity of the *Mecp2*$^{-/y}$ mice. While the sham and anti-leptin treated *Mecp2*$^{-/y}$ mice show similar phenotypic profile at the beginning of the treatment (p=0.43, Two-tailed unpaired *t*-test, **Figure 2C**), anti-leptin treated *Mecp2*$^{-/y}$ mice show better breathing parameters (number of apneas and breathing irregularity score) compared to sham *Mecp2*$^{-/y}$ mice at the end of the treatment (p=0.015 and 0.0015, Two-way ANOVA followed by a Bonferroni's multiple comparison, **Figures 2C, D and E, supplementary table 2**). The mean values of tidal volume (**data not shown**), respiratory frequency (**data not shown**) and minute ventilation (p>0.999, Two-way ANOVA followed by a Bonferroni's multiple comparison, **Figure 2F, supplementary table 5**) of P50 *Mecp2*$^{-/y}$ mice were not affected by the anti-leptin-treatment. We also tested the effect of leptin treatment and found no effect on the breathing parameters in *Mecp2*$^{-/y}$ mice (**Figures 2D, E and F, supplementary table 2**).

Altogether, these data suggest a contribution of leptin to the progression of breathing difficulties in symptomatic *Mecp2*$^{-/y}$ mice.

Leptin antagonism during the symptomatic stage prevents the worsening of health condition of *Mecp2*$^{-/y}$ mice.

We next assessed the efficacy of the anti-leptin treatment on the overall health of the *Mecp2*$^{-/y}$ mice. The thoroughly described loss in body weight in *Mecp2*$^{-/y}$ mice (p=0.00001, Two-tailed unpaired *t*-test **Figures 3A and B**, **supplementary table 3**) was abolished by the anti-leptin

treatment (5µg/g, every other day during 10 days, from P40 to P50) while the leptin-treated *Mecp2*$^{-/y}$ mice (5µg/g, 10 daily injections from P40 to P50) showed no difference compared to sham *Mecp2*$^{-/y}$ littermates (p=0.0001 and 0.59 respectively at P50, Two-way ANOVA followed by a Bonferroni's multiple comparison, **Figures 3B and C**, **supplementary table 3**). The leptin treatment also did not induce significant change in the body weight of the WT mice (p=0.06 at P50, Two-tailed unpaired *t*-test, **Figures 3C**, **supplementary table 3).** We also performed a general scoring of the health condition of the mice, including tremor, general aspect, spontaneous activity, limb grasp and posture. WT and *Mecp2*$^{-/y}$ mice showed significant difference at P40 (p=0.000001, two-tailed unpaired *t*-test, **Figure 3D, supplementary table 3**). The general health scoring performed on sham- and anti-leptin treated *Mecp2*$^{-/y}$ mice the day before the start of treatment (P40) and the last day of treatment (P50) revealed a deterioration of the health condition in sham *Mecp2*$^{-/y}$ mice that was not observed in anti-leptin treated *Mecp2*$^{-/y}$ mice (p=0.03 and 0.16, two-tailed paired *t*-test, **Figure 3E, supplementary table 3**). Improved symptoms are posture, tremor and general aspect while spontaneous activity and limb grasp showed no significant improvement (**Figure 3F, supplementary table 3**). Although it does not reach significance, this improvement in overall health of the anti-leptin treated *Mecp2*$^{-/y}$ mice was accompanied by a decrease of early lethality, with 50% of the sham- and anti-leptin treated *Mecp2*$^{-/y}$ mice surviving after the postnatal day 48.5 and 59 respectively (p=0.1, two-tailed unpaired *t*-test, p=0.16, Kaplan- Meier log rank test, **Figure 3G**). No lethality nor change in the health scoring were observed in WT mice treated with either vehicle or leptin (n=10 for both, data not shown).

We also assess the effect of the anti-leptin treatment on the locomotor activity and motor coordination of *Mecp2*$^{-/y}$ mice in the open field and the accelerating rotarod tests. In the open filed test, the distance traveled by the *Mecp2*$^{-/y}$ mice was reduced compare to their WT littermates (p=0.016, Two-tailed unpaired *t*-test **Figures 4A**, **supplementary table 7**). This locomotor deficit worsens with age in *Mecp2*$^{-/y}$ mice (p=0.03, P40 vs P50 *Mecp2*$^{-/y}$ sham, Two-tailed paired *t*-test, **Figures 4B**, **supplementary table 4**). The anti-leptin treatment (5µg/g, every other day during 10 days, from P40 to P50) prevented the degradation of locomotor activity of the *Mecp2*$^{-/y}$ mice (p=0.66, P40 vs P50 *Mecp2*$^{-/y}$ anti-leptin, Two-tailed paired *t*-test and p=0.04, P50 *Mecp2*$^{-/y}$ sham vs P50 *Mecp2*$^{-/y}$ anti-leptin, Two-tailed unpaired *t*-test, **Figures 4B and C**, **supplementary table 4**). Analysis of the behavior of the leptin-treated WT mice indicates that they performed similarly to their sham littermates (p=0.4, Two-tailed unpaired *t*-test **Figure 4C**, **supplementary table 4**). In the accelerating rotarod test, *Mecp2*$^{-/y}$ mice showed a significant decrease in the latency to fall compared to WT littermates (p<0.0001, Mann Whitney *U* test, **Figure 4D**, **supplementary table 7**). This phenotype did not worsen with age (p=0.29, P40 vs P50 *Mecp2*$^{-/y}$ sham, Wilcoxon matched pairs signed rank test, **Figures 4E**, **supplementary table 4**). Neither the leptin- nor the anti-leptin treatment affected the performances of respectively WT and *Mecp2*$^{-/y}$ mice on the accelerating rotarod test (p=0.18 and 0.42 respectively, two-tailed unpaired *t*-test, **Figure 4F, supplementary table 4**).

Overall, these observations show that the anti-leptin treatment ameliorates the overall health condition, i.e., posture, tremor and general aspect and locomotor activity of the symptomatic *Mecp2*$^{-/y}$ mice.

Leptin antagonism during the symptomatic stage does not affect anxiety in *Mecp2*$^{-/y}$ mice.

Leptin has been reported to exert anti-depressant and pro-cognitive like effects in rodents (Guo et al., 2012; Harvey, 2022). We therefore investigate the possible contribution of leptin to cognitive behavioral deficits repeatedly reported in RTT models (Kerr et al., 2010). Our first set of behavioral tests examined anxiety, cognition and social interaction in P50 WT and *Mecp2*$^{-/y}$ mice from our breeding colony. We first compared the spontaneous exploration in the elevated plus maze (EPM) as a measure of anxiety and found that *Mecp2*$^{-/y}$ mice spent more time in the open arms than their WT littermate ($p<0.0001$, Two-way ANOVA followed by a Bonferroni's multiple comparison, **Figure 4G**, **supplementary table 4**). The mean dipping time was also increased in *Mecp2*$^{-/y}$ mice ($p=0.086$, Two-way ANOVA followed by a Bonferroni's multiple comparison, **Figure 4H**, **supplementary table 4**) a behavior also consistent with decreased anxiety. However, no genotype effects were found in tests used to evaluate object recognition and social behavior (**supplementary Figure S1, supplementary table S1**). We therefore limited the study of the role of leptin to the EPM. Analysis of the behavior of the leptin-treated WT and anti-leptin treated-*Mecp2*$^{-/y}$ mice in the EPM indicates that they performed similarly to their vehicle-treated WT littermate, i.e. they stayed similar time in the open arms and exhibited similar mean dipping time (**Figures 4H and G**, **supplementary table 4**).

Overall, these observations show that the anti-leptin treatment does not improve anxiety impairment in the symptomatic *Mecp2*$^{-/y}$ mice.

Symptomatic leptin antagonism does not improve seizures susceptibility in *Mecp2*$^{-/y}$ mice.

Seizures are predominant features in RTT patients and abnormal cortical activities have been observed in *Mecp2*-deficient mice (Glaze, 2002; D'Cruz et al., 2010). Leptin modulates the excitability of neuronal networks and exerts both anti-convulsant and pro-convulsant effects

(Mora-Muñoz et al., 2018). To gain insight into the possible contribution of leptin in RTT-associated epileptic activity, we challenged P50 *Mecp2*$^{-/y}$ mice and their WT littermates with the volatile convulsant agent flurothyl (2,2,2-trifluoroethyl ether). Flurothyl induced severe tonic-clonic seizures with a loss of posture in both WT- and *Mecp2*$^{-/y}$ mice. The onset of seizures was more rapid in *Mecp2*$^{-/y}$ mice as compared to their WT littermates (p=0.0007, Two-tailed unpaired *t*-test, **Figure 5A, supplementary table 5**). Moreover, all *Mecp2*$^{-/y}$ mice died after the tonic-clonic seizures, while lethality was observed in 44% of WT mice (p=0.0029, Fisher exact test, **Figure 5C**). We next investigated the effect of daily leptin treatment (0.5µg/g during 10 consecutive days) on the seizure latency in WT mice and found no significant difference in seizure latency (p=0.34, Two-tailed unpaired *t*-test, **Figure 5B, supplementary table 5**) and lethality (p>0.999, Fisher exact test, **Figure 5D**) compared to WT sham WT. Similarly, neither the leptin- nor the anti-leptin (0.5µg/g, every other day during 10 days) treatments affected flurothyl-induced seizures latency (p>0.999 for both, two-way ANOVA followed by a Bonferroni's multiple comparison) and lethality (p>0.999 for both, Fisher exact test) in *Mecp2*$^{-/y}$ mice (**Figures 5B and D, supplementary table 5)**.

Altogether, these data suggest that leptin does not contribute to seizure susceptibility in symptomatic *Mecp2*$^{-/y}$ mice.

Leptin antagonism during the symptomatic stage restores the E/I balance in CA3 hippocampal neurons in *Mecp2*$^{-/y}$ mice.

We then assessed the potential benefits of anti-leptin treatment at the neuronal level. Alteration in the synaptic excitation/inhibition (E/I) balance is a widespread feature of neuronal networks in *Mecp2*-deficient mice (Li, 2022). Leptin has been reported to modulate the development and

functioning of both glutamatergic and GABAergic hippocampal synapses (Moult and Harvey, 2009; Dhar et al., 2014; Guimond et al., 2014; Dumon et al., 2018; Sahin et al., 2020, 2021; Harvey, 2022), raising the possibility that elevated leptin levels might contribute to the altered E/I balance in *Mecp2*$^{-/y}$ mice. We therefore performed whole cell patch clamp recordings of CA3 pyramidal neurons performed on acute hippocampal slices obtained from WT and *Mecp2*$^{-/y}$ mice and found that, as already reported (Calfa et al., 2015; Lozovaya et al., 2019), the E/I balance was increased at both presymptomatic (0.9±0.2 vs 4.5±0.9 in respectively P30 WT (10 cells, 3 mice) and *Mecp2*$^{-/y}$ (13 cells, 3 mice) mice littermates, p=0.014, Two-tailed Mann-Whitney test, **data not shown**) and symptomatic stages (p<0.0001 at P50, Two-tailed Mann Whitney test, **Figures 6A, B and D, supplementary table 6**). We next assed the effect of the leptin and leptin antagonism treatment on the E/I balance. The leptin treatment (0.5µg/g during 10 consecutive days from P40 to P50) led to a significant increase in the E/I balance in P50 WT mice, thus phenocopying the *Mecp2*$^{-/y}$ mice (p=0.014, Two-tailed Kruskal-Wallis test followed by Dunn's post hoc comparison, **Figure 6C, supplementary table 2).** This increase in the E/I balance is mainly accounted for by a reduction of GABAergic activity (p=0.002, **Figure 6E, supplementary table 6**). When administered to *db* mice (mice deficient for the long-form leptin receptor, the only receptor capable of activating intracellular pathways (Ahima and Flier, 2000)), leptin had no effect on the E/I balance (1.57±0.3 vs 1.58±0.3 for respectively *db*-sham (13 cells, 2 mice) and *db*-lep (9 cells, 2 mice), p=0.787, Two-tailed Mann-Whitney test) and GABAergic activity (26.5±6.1 vs 20.6+4.1 Hz, p=0.638, Two-tailed Mann-Whitney test, **data not shown)**. In contrast to leptin treatment, the anti-leptin treatment (0.5µg/g every other day from P40 to P50) had no effect on the E/I balance of WT mice (p>0.999 when compared to WT-sham, Two-tailed Kruskal-Wallis test followed by Dunn's post hoc comparison**, supplementary table 6**). Treatment of *Mecp2*$^{-/y}$ mice revealed that leptin had no significant effect on the E/I balance

(p=>0.999, Two-tailed Kruskal-Wallis test followed by Dunn's post hoc comparison**, Figure 6C, supplementary table 6**). In contrast, the anti-leptin treatment restored the E/I balance in *Mecp2*$^{-/y}$ mice (p=0.005 when compared to Mecp2$^{y/-}$-sham, p>0.9999 when compared to WT-sham, Two-tailed Kruskal-Wallis test followed by Dunn's post hoc comparison, **Figure 6C, supplementary table 6**) and increased the GABAergic activity (p=0.028 when compared to *Mecp2*$^{-/y}$-sham, p>0.9999 when compared to WT-sham, Two-tailed Kruskal-Wallis test followed by Dunn's post hoc comparison, **Figure 6E, supplementary table 6**).

Altogether, these data show that the leptin-treatment increases the E/I balance in WT mice phenocopying the *Mecp2*$^{-/y}$ mice, while the anti-leptin treatment rescues the E/I balance in *Mecp2*$^{-/y}$ mice. These observations suggest a contribution of leptin to the hippocampal E/I imbalance in symptomatic *Mecp2*$^{-/y}$ mice.

Leptin antagonism during the symptomatic stage restores the hippocampal synaptic plasticity in *Mecp2*$^{-/y}$ mice.

Impairments of synaptic plasticity are common features of mice RTT models (Asaka et al., 2006; Moretti et al., 2006; Lozovaya et al., 2019) and leptin has been reported to modulate the strength of glutamatergic synapses (McGregor and Harvey, 2019). These observations prompted us to examine the effect of leptin and leptin antagonist treatment on long term potentiation (LTP) at the hippocampal Schaffer collaterals-CA1 synapses of P50 WT and *Mecp2*$^{-/y}$ mice. Field EPSPs were recorded in the stratum radiatum and evoked by stimuli of increasing strength. The slope of the input-output curves obtained from *Mecp2*$^{-/y}$ mice were not significantly different from WT littermates showing that the basal neurotransmission at the Schaffer collateral-CA1 synapses is unaltered in symptomatic *Mecp2*$^{-/y}$ mice (the slope of curve afferent volley amplitude vs field

EPSP slope was 5.1±0.7 vs 5.2±0.7 in respectively WT and *Mecp2*$^{-/y}$ mice, p=0.8, Mann Whitney *U* test, data not shown). Next, LTP was induced by two trains of 100 Hz tetanic stimulation (1 sec duration, 20 sec interval). As already reported (Asaka et al., 2006), the magnitude of LTP was reduced in *Mecp2*$^{-/y}$ compared to WT littermates (p=0.012 at 45-50 min post-tetanus, repeated measure ANOVA, **Figure 7A, supplementary table 7**). The magnitude of potentiation in the first minutes following the tetanic stimulation was also reduced (p=0.08 at 0-2 min post-tetanus, repeated measure ANOVA, **Figure 7A, supplementary table 7**). Leptin treatment of WT mice (5µg/g during 10 consecutive days from P40) attenuated the magnitude of late and early LTP compared to sham-treated but these differences did not reach significance (p=0.16 and 0.27 for the early and late LTP, repeated measure ANOVA, **Figure 7B, supplementary table 7**). Conversely, the anti-leptin treatment (0.5µg/g every other day during 10 days from P40) restored the magnitude of early and late LTP in *Mecp2*$^{-/y}$ mice (p=0.08 and 0.03 respectively, repeated measure ANOVA, **Figure 7C, supplementary table 7**).

Altogether, these data suggest that leptin contributes to the impairment of hippocampal LTP in symptomatic *Mecp2*$^{-/y}$ mice.

RTT-associated symptoms are improved in leptin haplo insufficient mice.

To further evaluate the possible contribution of leptin in RTT phenotype, we generated *Mecp2*$^{-/y}$ mice that are haplo insufficient for leptin. For this, female *Mecp2*$^{+/-}$ mice were backcrossed with heterozygous leptin deficient male mice (*ob*/+). The resulting double transgenic *Mecp2*$^{-/y;ob/+}$ mice showed normalized leptin levels at P50-60 (p=0.8 compared to WT mice, Two-way ANOVA followed by a Bonferroni's multiple comparison, **Figure 8A**, **supplementary table 8**). We next asked whether the RTT associated deficits were ameliorated in these leptin haplo

insufficient mice at P50-60, an advanced symptomatic stage. Whole cell recordings performed on hippocampal slices revealed that the E/I balance and sGABA-PSCs frequency are improved in CA3 hippocampal neurons of *Mecp2*$^{-/y;ob/+}$ mice (p=0.39 and 0.02 respectively when compared to WT mice, **Figure 8A and C**, **supplementary table 8**). Field recordings on hippocampal slices further revealed that the magnitude of early and late LTP at the Schaffer collateral-CA1 synapses was increased in *Mecp2*$^{-/y;ob/+}$ mice (p=0.08 and 0.05 respectively when compared to *Mecp2*$^{-/y}$ mice, **Figure 8D**, **supplementary table 8**). The *Mecp2*$^{-/y;ob/+}$ mice also showed improved breathing activity (p=0.002 when compared to WT, **Figure 8E**, **supplementary table 8)** and less weight loss (p=0.05 when compared to WT, **Figure 8F**, **supplementary table 8**).

Overall, these data show that reduced leptin production improves the symptoms of *Mecp2*$^{-/y}$ mice.

DISCUSSION

Here, we show that *Mecp2*$^{-/y}$ mice have elevated circulating leptin levels and leptin mRNA expression compared to their age-matched WT littermates. Knowing the pleiotropic central and peripheral roles of leptin, this finding provided a framework for investigating the possible contribution of this adipocyte hormone in RTT pathogenesis. We thus tested the rescue potential of leptin antagonism approaches. We found that 10-day treatment from P40 of male *Mecp2*-null mice with a leptin antagonist prevents the worsening of several symptoms including breathing difficulty, locomotor deficit, weight loss and degradation of general health condition. At the neuronal level, the anti-leptin treatment restores the E/I balance and synaptic plasticity in the hippocampus. A further validation of our hypothesis is the benefits observed in mice haplo insufficient for leptin (*Mecp2*$^{-/y;ob/+}$ mice). The leptin antagonism strategy was however ineffective against seizure susceptibility, anxiety and motor coordination deficit. In line with the contribution of leptin to RTT pathogenesis, we showed that leptin treatment of WT mice induces hippocampal E/I imbalance, reduces hippocampal synaptic plasticity and causes breathing abnormality, thus phenocopying some RTT symptoms.

Previous studies found that leptin concentrations were increased in patients with Rett syndrome, but not associated with increases in weight gain or body mass index (Blardi et al., 2007, 2009; Acampa et al., 2008). Elevated leptin level could be related to chronic inflammatory state due to frequent respiratory infections (Cortelazzo et al., 2014) as well as hormonal and/or metabolic deregulations (Motil et al., 2011; Stagi et al., 2015). Medications, such as anticonvulsants, can also alter circulating leptin levels in patients (Belcastro et al., 2013). However, according to previous studies (Park et al., 2014; Fukuhara et al., 2019), we showed that

342 *Mecp2*-null mice also present elevated levels of circulating leptin, even though they did not
343 receive any medication. This leptin elevation was observed in males in different models and
344 genetic backgrounds as well as in female *Mecp2*$^{+/-}$ mice (Park et al., 2014; Torres-Andrade et al.,
345 2014; Fukuhara et al., 2019) (present study and unpublished observations) highlighting the
346 robustness of this finding and its possible relevance to the clinical situation. The mechanism
347 underlying the increase in leptin protein and mRNA levels observed in *Mecp2*-deficient mice is
348 presently unknown but likely rely on non-cell autonomous mechanisms since (i) neuron-specific
349 Mecp2 knockout mice (*Mecp2*$^{tm1.1Jae}$ KO mice) showed increased circulating leptin levels and
350 WAT leptin mRNA expression (Park et al., 2014) and (ii) adipocyte-specific Mecp2 knockout
351 mice (*Mecp2*^{Adi} KO mice) showed down regulated WAT leptin mRNA expression and similar
352 circulating leptin levels compared to WT mice (Liu et al., 2019). An increase in WAT mass
353 could explain the elevated leptin levels in *Mecp2*-deficient mice. Previous studies have shown
354 that Lep mRNA expression and circulating leptin levels are increased in *Mecp2*-deficient mice
355 (Torres-Andrade et al., 2014) and POMC neuron-specific Mecp2 knockout mice (Wang et al.,
356 2014) in association with an increase in body weight. Two other studies reported elevated leptin
357 levels in *Mecp2*-deficient mice without weight change but with increased WAT mass (Park et al.,
358 2014; Fukuhara et al., 2019). In the present study, WAT mass was not measured, but it is worth
359 noting that the progressive increase in leptin levels and leptin mRNA expression were observed
360 despite a decline in body weight. Adipose tissue is also present within skeletal muscle.
361 Intramuscular adipose tissue (IMAT) accumulation is observed in pathological conditions such as
362 muscle dystrophy, obesity and metabolic diseases (Sciorati et al., 2015). IMAT accumulation
363 may underlie elevated leptin mRNA expression in muscle of symptomatic male *Mecp2*-null mice,
364 which exhibit hypotrophic fibres and tissue fibrosis (Conti et al., 2015).

We have shown that pharmacological leptin antagonism and genetic reduction of leptin production ameliorate some RTT phenotype and prevent the degradation of others in symptomatic male *Mecp2*-null mice. We used a pegylated super active mouse leptin antagonist (Peg-SMLA). This antagonist poorly penetrated in the central nervous system, and inhibits leptin activity by two mechanisms: (i) by blocking the transport of circulating leptin across the blood brain barrier (BBB), thus reducing central leptin levels, and (ii) by blocking the binding of leptin to its peripheral receptors, thus reducing peripheral leptin signaling (Elinav et al., 2009). Likewise, haplo insufficiency for leptin will reduce both central and peripheral actions of leptin in *Mecp2*$^{-/y;ob/+}$ mice. Several observations support the hypothesis that the beneficial action of leptin antagonism relies on a reduction in the central action of leptin. First, functional leptin receptors are expressed throughout the brain (Caron et al., 2010). Then, *in vitro* studies indicate that leptin directly regulates the excitability and synaptic function of neurons within different brain regions including the hippocampus (Shanley et al., 2002; Harvey et al., 2006; Solovyova et al., 2009; Dhar et al., 2014; Guimond et al., 2014; Dumon et al., 2018; Sahin et al., 2021) and nucleus tractus solitarii, a crucial site for the modulation of breathing, cardiovascular control and food intake (Williams and Smith, 2006; Neyens et al., 2020; Yu et al., 2022). Lastly, *in vivo* experiments show that local/systemic injections of leptin, as well as chemogenetic/optogenetic activation of leptin receptor expressing neurons, modulate physiological and behavioral responses, and that targeted deletion of central leptin receptors prevent these effects (Oomura et al., 2006; Inyushkin et al., 2009; Vong et al., 2011; Guo et al., 2013; Zuure et al., 2013; Bassi et al., 2014, 2015; Yu et al., 2022). The respiratory network is complex and the effects of leptin on respiratory control are still poorly understood. However, alterations in the E/I balance have been

388 reported in respiratory nuclei that express leptin receptor such as the nucleus tractus solitarius and
389 the rostro ventrolateral medulla (Medrihan et al., 2008; Chen et al., 2018). The latter could
390 contribute to apneustic and irregular breathing in *Mecp2*-deficient mice (Ramirez et al., 2013).
391 Additional work is required to determine whether and how leptin antagonisms affect the E/I
392 balance in these brain regions, but also in cortical areas where the E/I balance is reduced (Li,
393 2022). Finally, we cannot completely rule out a peripheral effect of treatments in addition to the
394 central effect, acting for example on carotid bodies.

395

396 Knowing the facilitatory role of leptin on breathing and synaptic function, the present
397 finding might seem counter-intuitive. It is however worth noting that an excess of leptin can lead
398 to a blunted response to leptin, a condition known as “leptin resistance”. Thus, rodents fed with a
399 high-fat diet that causes elevated leptin levels and leptin resistance also show altered
400 hippocampal synaptic function, breathing difficulties and changes in anxiety level (Grillo et al.,
401 2011; Valladolid-Acebes et al., 2012; Farr et al., 2015; Gauda et al., 2020). It cannot be totally
402 excluded that the anti-leptin treatment or the haplo insufficiency for leptin, by decreasing the
403 central levels of leptin, reduces the phenomenon of resistance and allows leptin to exert its
404 beneficial effects. Similarly, leptin treatment of WT mice could lead to leptin resistance, which
405 would be responsible for the symptoms observed in these mice. Elevated leptin levels have also
406 been observed in children with autism spectrum disorders (Ashwood et al., 2008; Blardi et al.,
407 2010; Raghavan et al., 2018). Yet, the clinical features seen in ASD do not completely overlap
408 those broader of Rett syndrome, suggesting that the functional and physiological actions of leptin
409 may depend, among other things, on the mutations associated with the etiology of the disease, in
410 the present situation of the Mecp2 mutations.

411 The success of most genetic and pharmacological therapeutic approaches relies on the
412 ability of the virus or drugs to cross the BBB. To overcome this difficulty, we have used a
413 competitive antagonist of leptin whose main action is to block the transport of leptin across the
414 BBB (Elinav et al., 2009). We have shown that the treatment is well tolerated (no premature
415 death during the treatment, no overt side effect) holding potential therapeutic application.
416 Moreover leptin antagonist therapy has been reported to be efficient for the prevention or
417 treatment of diseases in which high leptin levels is part of the picture (Singh et al., 2013; Fisch et
418 al., 2020). It is noteworthy that leptin antagonist treatment also improves bone mineralization
419 (Chapnik et al., 2013) and muscle function (Gonzalez et al., 2021), two peripheral symptoms
420 observed in RTT. Furthermore, hyperleptinemia has been proposed to play a role in sympathetic
421 over activity and cardiac abnormalities observed in RTT (Acampa et al., 2008). Overall, these
422 observations suggest that leptin might participate to RTT clinical manifestations other than
423 central synaptic activity, breathing and weight loss, highlighting the global therapeutic interest of
424 this approach.

425

426 Given the progressive nature of Rett symptoms and the high inter-individual variability,
427 we assessed their evolution (i.e., the difference between the values at the beginning and at the end
428 of treatment) to estimate the potential efficacy of the leptin antagonist treatment. Our data show
429 that treatment with the leptin antagonist in the symptomatic period delays the progression of
430 certain symptoms (i.e. breathing, locomotor activity, weight loss, general health status) rather
431 than curing them. The performance to rotarod, which does not show any degradation in the
432 studied period, was not modified. The notion of a "pre-symptomatic" period in RTT has recently
433 been questioned by studies showing subtle symptoms in RTT girls and early alterations in animal

models before the appearance of overt symptoms (Cosentino et al., 2019). Therefore, even if translational applications would be difficult, it will be interesting in the future to determine whether pre-symptomatic treatments have greater positive effects.

MATERIALS and METHODS

Animals

All animal procedures were carried out in accordance with the European Union Directive of 22 September (2010/63/EU) and have been approved by the Ethical Committee for Animal Experimentation (APAFIS-Number 17605-2018-1119-1115-7094) delivered by the French Ministry of Education and Research.

Experiments were performed on male wild type and *Mecp*$^{2tm1\text{-}1Bird}$ mice (Guy et al., 2001) C57BL/6 genetic background (Jackson Laboratory, stock number 003890). Hemizygous mutant males (hereafter referred as to *Mepc2*$^{-/y}$ mice) were generated by crossing heterozygous females (*Mecp2*$^{+/-}$) with C57BL/6 wild type males. *Mecp2*$^{-/y}$ mice haplo insufficient for leptin (hereafter referred as to *Mecp2*$^{-/y;ob/+}$) were generated by crossing heterozygous females *Mecp2*$^{+/-}$ with C57BL/6 heterozygous leptin deficient males mice (Jackson Laboratory genotyping protocol, strains B6.Cg-Lepob/J, ID 000632). Animals were housed in a temperature-controlled environment with a 12h light/dark cycle and free access to food and water. Genotyping was performed by PCR techniques according to Jackson Laboratory protocols.

Leptin and anti-leptin injection

Recombinant murine leptin (Peprotech, New Jersey, USA) was reconstituted in sterile water and daily injected (5 µg/g) sub-cutaneous at 12-14 hr a.m during 10 days starting at postnatal (P) 40. The pegylated super active mouse leptin antagonist (Peg-SMLA, Protein Laboratories, Rehovot, Israel) was reconstituted in sterile water (Elinav et al., 2009; Gertler and Elinav, 2014). As the

460 half-life of the Peg-SMLA was about 24 hours, mice were injected (5 µg/g) sub-cutaneous at 12-
461 14 hr a.m every other day during 10 days starting at P40. Control mice received same volume
462 injections of vehicle.

463

464 **Leptin immunoassay**

465 Blood samples were centrifuged (10.000 rpm, 10 min, 4°C) immediately after collection at 10–11
466 hr a.m. Quantification of endogenous leptin was performed with Mouse Leptin ELISA Kit
467 (BioVendor R&D^{R}, Brno, Czech Republic) following the manufacturer's protocol. The measured
468 concentration of samples was calculated from the standard curve and expressed as ng/ml.

469

470 **Real-time reverse transcription quantitative polymerase chain reaction**

471 Visceral and inguinal fat pads and gastrocnemius muscles were dissected, rapidly frozen in liquid
472 nitrogen and stored at -80°C. Total RNAs from fat pads and gastrocnemius muscle were isolated
473 using a RNeasy Mini kit (74106, Qiagen, Germany) and RNA Fibrous Tissue Mini kit (74704,
474 Qiagen) respectively, following the manufacturer's instructions and quantified by reading the
475 absorbance at 260 nm (NanoPhotometer, IMPLEN). RNAs were converted to cDNA using 1 µg
476 RNA and a QuantiTect Reverse Transcription kit (Qiagen) according to manufacturer's
477 instructions. Quantitative RT-PCR was performed with a Light Cycler 480 SYBR Green IMaster
478 (Roche Applied Science) following the manufacturer's instructions, using the following
479 oligonucleotides (QuantiTect Primer Assays, Qiagen): Leptin (Mm_Lep_1_SG QT00164360
480 (NM_008493)), and glyceraldehyde-3-phosphate dehydrogenase (GAPDH, QT001199633).

Relative mRNA values were calculated using the LC480 software and GAPDH as the housekeeping gene. PCR was performed in triplicate.

Hippocampal slice preparation and electrophysiological recordings

Brains were removed and immersed into ice-cold (2° to 4°C) artificial cerebrospinal fluid (ACSF) with the following composition: 126 mM NaCl, 3.5 mM KCl, 2 mM CaCl2, 1.3 mM MgCl2, 1.2 mM NaH2PO4, 25 mM NaHCO3, and 11 mM glucose (pH 7.4) equilibrated with 95% O2 and 5% CO2. Hippocampal slices (350µm thick) were cut using a vibrating microtome (Leica VT1000S, Germany) in ice-cold oxygenated choline-replaced ACSF and were allowed to recover at least 90 min in ACSF at room temperature (25°C). Slices were then transferred to a submerged recording chamber perfused with oxygenated (95% O2 and 5% CO2) ACSF (3 ml/min) at 34°C.

Whole cell recordings were performed from CA3 pyramidal neurons in the voltage-clamp mode using an axopatch 200B amplifier (Molecular Devices LLC, San Jose, USA). To assess the excitatory/inhibitory balance, the glass recording electrodes (4-7 MΩ) were filled with a solution containing 100 mM K-gluconate, 13 mM KCl, 10 mM Hepes, 1.1 mM EGTA, 0.1 mM CaCl2, 4 mM Mg–adenosine 5′-triphosphate, and 0.3 mM Na–guanosine 5′-triphosphate. The pH of the intracellular solution was adjusted to 7.2, and the osmolality was adjusted to 280 mOsmol liter−1. With this solution, $GABA_A$-receptor mediated postsynaptic currents ($GABA_A$-PSCs) reversed at −70 mV. $GABA_A$-PSCs and Glut-PSCs were recorded at a holding potential of −45 and -70 mV respectively. Spontaneous synaptic currents, were recorded with Axoscope software version 8.1 (Molecular Devices LLC, San Jose, USA) and analyzed offline with Mini Analysis Program version 6.0 (Synaptosoft).

Field recordings were performed in area CA1. A cut was made between CA1 and CA3. The Schaffer collaterals/commissural fibers were stimulated using a bipolar tungsten electrode (66 µm; A-M Systems, WA, USA) placed on the surface of the stratum radiatum of CA1 (10–50 µs, 5–15 V, 0.03 Hz). Extracellular tungsten electrodes (California Fine Wire,CA, USA) were used to record dendritic field excitatory postsynaptic potentials (fEPSP) from the stratum radiatum of the CA1 region. The signals were amplified using a DAM80 amplifier (WPI, UK), digitized with an Axon Digidata 1550B (Molecular Devices, CA, USA), recorded with Axoscope software version 8.1 (Molecular Devices, CA, USA) and analyzed offline with Mini Analysis Program version 6.0 (Synaptosoft, GA, USA) by measuring the onset (a 30–70% rising phase) slope of the fEPSP. LTP was induced by two 100 Hz trains of 100 stimuli 20 sec apart at 50% of the maximal intensity. The slope of the fEPSP was measured and expressed relative to the preconditioning baseline.

Plethysmography.

The breathing activity of non-anesthetized freely moving mice was recorded using a constant flow whole body plethysmograph (EMKA technologies, Paris, France) with 200ml animal chambers maintained at 25±0.5 ˚C and ventilated with air (600ml min-1). The breathing activity of pairs of WT and *Mecp2*$^{-/y}$ mice littermates was simultaneously recorded. Mice were allowed to acclimate to the experimental room for 1 hour and to the plethysmography chamber and airflow for approximatively 30 mins before breathing measurement. Breathing activity was recorded during 1 hour. A differential pressure transducer measured the changes in pressure in the body chamber resulting from the animal's respiration. Signals from the pressure transducer were stored on a personal computer and analyzed offline via the Spike 2 interface and software (Cambridge

Electronic Design, Cambridge, UK). Only periods of quiet breathing without body movements were analyzed, during which the number of apneas (> two respiratory cycles) per hour was quantified.

Fluorothyl-induced seizures

To test seizure susceptibility, we used the convulsant agent flurothyl (2,2,2-trifluoroethyl ether). P50-55 male mice were placed in a transparent, ventilated but hermetically sealed, cage, into which the epileptic agent flurothyl was delivered at a rate of 25nl/min using a nano-pump (Harvard Apparatus) and homogeneously distributed using a mini-ventilator incorporated into the chamber. Behavioral responses were recorded using a video camera. The latency of tonic-clonic seizures was determined post hoc. The progressive injection of flurothyl into the cage produced a stereotypical behavioral manifestation of limbic seizure episodes that started from animal immobility, followed by intermediate stages (rigid posture, tranquility period, jiggles, and jerks) and ended by severe tonic-clonic seizures (stage 4). The injection of flurothyl was stopped ten seconds after beginning of tonic-clonic seizures and the cage was ventilated with fresh air. Some mice regain motor and exploratory activity after 10 mins. Others die during the tonic seizures. The percentage of surviving/dying mice varies according to the genotype and the treatment (see results section).

General health scoring and lifespan

Weight was measured every day from the beginning of the treatment. The phenotypic score was evaluated the day before treatment and the last day of treatment. Severity score, typically used in

RTT phenotypic assessments (Guy et al., 2001; Scaramuzza et al., 2021), was used to group animals into 4 severity classes: absence of phenotype (4) to severe phenotype (0). The parameters scored are: tremor, posture, limb grasp, spontaneous activity in the home cage and general aspect. To be noticed, mice that rapidly lost weight were euthanized for ethical reasons. The day of the sacrifice was considered as the endpoint of lifespan assessment.

Accelerating rotarod

A rotarod apparatus (Biological Research Apparatus, Gemonio, Italy) was used to measure the motor coordination. After a 5 mins habituation session (4 r.p.m), each mouse was given three trials with the rate of rotation increasing from 4 to 40 r.p.m. over 5 mins. The trial ended when the mouse fell from the rod or remained on the rotarod for at least 5 mins. The time spent on the rotarod was recorded by an automated unit, which stopped as the mouse fell. The mouse was placed back in its home cage for 10 mins between each trial. The latency to fall was determined as the best of the 3 trials.

Behavior

All the behavioral tests were performed by Phenotype Expertise, Inc. (France). For all tests, animals were first acclimated to the behavioral room for 30 minutes. WT and *Mecp2*$^{-/y}$ mice underwent elevated plus maze, open field, three chamber test and spontaneous social interaction test at P50. WT and *Mecp2*$^{-/y}$ treated mice underwent elevated plus maze and open field at P40, before the beginning of the treatment, and at P50, at the end of the treatment.

571 *Elevated-Plus Maze.* The EPM was used to assess anxiety state of animals. The device consists of
572 a labyrinth of 4 arms 5 cm wide located 80 cm above the ground. Two opposite arms are open
573 (without wall) while the other two arms are closed by side walls. The light intensity was adjusted
574 to 20 Lux on the open arms. Mice were initially placed on the central platform and left free to
575 explore the cross-shaped labyrinth for 5 minutes. Maze was cleaned and wiped with H2O and
576 with 70% ethanol between each mouse. Animal movement was video-tracked using Ethovision
577 software 11.5 (Noldus). Time spent in open and closed arms, the number of entries in open arms,
578 as well as the distance covered, are directly measured by the software.

579

580 *Open-field.* Open field was used to evaluate both the locomotor activity of the animals. Mice
581 were individually placed in a 40 x 40 cm square arena with an indirect illumination of 60 lux.
582 Mouse movement was video-tracked using Ethovision software 11.5 (Noldus) for 10 minutes.
583 Total distance traveled and time in center (exclusion of a 5 cm border arena) are directly
584 measured by the software. Grooming (time and events) and rearing were manually counted in live
585 using manual functions of the software, by an experimented behaviorist. The open-field arena
586 was cleaned and wiped with H2O and with 70% ethanol between each mouse.

587

588 *Three-chamber social preference test.* The test was performed as described previously (Bertoni et
589 al., 2021) with the following modifications to accommodate for the lower mobility of the
590 animals. A square arena 40 x 40 cm was used, with the wired cages placed in opposite diagonal
591 corners. The task was carried out in four trials. The three-chambers apparatus was cleaned and
592 wiped with water and with 70% ethanol between each trial and each mouse. In the first trial
593 (habituation), a test mouse was placed in the center of the arena and was allowed to freely

explore each chamber. The mouse was video-tracked for 5 min using Ethovision software. At the end of the trial, the animal was briefly removed from the arena to allow for the preparation of the following trial. In the second trial (social exploration), a 8- weeks old C57BL/6J congener mouse (S1) was placed randomly in one of the two wire cages to avoid a place preference. The second wire cage remained empty (E). Then the test mouse was placed in the center of the arena and allowed to freely explore for 10 min. A second 8-weeks old C57BL/6J congener mouse (S2) was placed in the second wire cage for the third trial (social discrimination). Thus, the tested mouse had the choice between a familiar mouse (S1) and a new stranger mouse (S2) for 10 min. At the end of the trial, the mouse was returned to home-cage for 30 min. For the fourth trial (short-term social memory), S2 was replaced by a new stranger mouse (S3), the familiar mouse (S1) staying the same. Then tested mouse was allowed to freely explore the arena for 10 min. Time spent in each chamber and time of contact with each wire cage (with a mouse or empty) were calculated using Ethovision software. The measure of the real social contact is represented by the time spent in nose-to-nose interactions with the unfamiliar or familiar mouse. This test was performed using grouped house mice of 4 months old.

Spontaneous social interaction test. The tested mouse was placed into the same OF arenas that were used for the OF test and allowed to explore this empty arena for 2.5 min. Immediately following this initial stage, the mouse was again allowed to explore the OF for an additional 10 min with the target (Swiss mouse) present. Mouse movement was video-tracked using Ethovision software 11.5 (Noldus) and the time spent in nose-to-nose, nose-to-body, and nose-to-genitals interactions was measured.

Statistics

Statistical analyses were conducted with GraphPad Prism (GraphPad software 5.01). Shapiro-Wilk normality test was used to determine the normality of distributions. We used a Two-tailed Mann-Whitney *U* test or Two-tailed unpaired *t*-test for comparison between two independent groups, a Wilcoxon matched pairs signed rank test or Two-tailed paired *t*-test for comparison between two matched data, a Two-tailed Kruskal-Wallis test followed by a Dunn's multiple comparison or a two-way ANOVA followed by a Bonferroni's multiple comparison for comparison between three or more independent groups, and a Fisher exact test for nominal comparison between two independent groups. The effect of tetanic stimulation of the slope of field EPSPs was analyzed using repeated measure ANOVA. The survival analysis was performed using a Kaplan-Meier log-rank test. Possible outliers within an experimental group were identified with Grubb's test and discarded from the final analysis. To ensure the consistency and reproducibility of our results, we conducted repeated trials in different acute hippocampal slices prepared from at least three different animals from three different littermates. All data are expressed as mean $\pm$ standard error to the mean (S.E.M.). For results expressed as percent of WT (i.e. serum and mRNA leptin, Figure 1, all values (WT and *Mecp2*$^{-/y}$ mice) were normalized to the mean WT value. In the figures, box plots represent the 1^{rst} and 3rd quartiles; whiskers show data range; horizontal lines show the median.

ACKNOWLEDGMENTS

We thank the members of the Molecular and Cellular Biology facility and Animal facility at INMED. We thank Drs F. Muscatelli and I. Medyna for critical reading of the manuscript.

CONFLICT OF INTEREST STATEMENT

The authors declare no conflict of interest.

DATA AVAILABILITY

All datasets generated for this study are available on request to the corresponding author.

AUTHOR CONTRIBUTIONS

J-LG, YB, CM and GAW conceived the experiments and wrote the manuscript. YB, J-LG, DD, MB-H and VV performed the experiments. CS performed the behavioral analysis. J-CG bred the colony. All authors approved the final version of the manuscript.

FUNDING

This work was supported by the National Institute of Health (Grant 1R01HD092396), the Association Française du Syndrome de Rett, INSERM Transfert, Fondation Lejeune, and the Excellence Initiative of Aix-Marseille University-A*midex, a french “Investissements d’Avenir programme”, MarMara AMX-19-IET-007.

FIGURE LEGENDS

Figure 1: Circulating leptin levels and leptin mRNA expressions are elevated in symptomatic *Mecp2*$^{-/y}$ mice.

A) Box plots of serum leptin levels determined in blood samples taken at postnatal day (P) 15, 30 and 50, using ELISA kit and expressed as percentage of age matched wild type (WT) mice mean. **B)** Scatter plots of serum leptin levels as a function of mice body weight of P30-P50 WT and *Mecp2*$^{-/y}$ mice. **C**) Box plots of normalized Leptin mRNA expression in gastrocnemius muscle of P30 and P50 WT and *Mecp2*$^{-/y}$ littermates. **D, E**) Box plots of normalized Leptin mRNA expression in the visceral (V) and inguinal (In) white adipose tissue (WAT) of P30 and P50 WT and *Mecp2*$^{-/y}$ littermates. In this and following figures, box plots represent quartiles, whiskers show data range, lozenges represent arithmetic means. Numbers in parentheses indicate the number of mice used. *P < 0.05, **P < 0.01, ***P < 0.001, two-tailed unpaired student *t*-test.

Figure 2: Leptin antagonism prevents the progression of breathing deficits of symptomatic *Mecp2*$^{-/y}$ mice.

A) Box plots of apnea frequency in P40 untreated WT and *Mecp2*$^{-/y}$ mice. **B, C**) Plots of apnea frequency in untreated and treated WT (**B**) and *Mecp2*$^{-/y}$ (**C**) mice. Lines indicate individual mice recorded the day before the treatment (P40) and at the end of the treatment (P50). Connected scares indicate mean±SEM. **D-F**) Box plots of the percentage of change of apnea frequency (**D**), breathing irregularity score (**E**) and minute ventilation (**F**) in sham- and treated- WT and *Mecp2*$^{-/y}$ mice. Numbers in parenthesis indicate the number of mice used. $^{**}P < 0.01$; $^{***}P < 0.001$, Two-tailed paired t-test (B, C), Two-tailed unpaired t-test (D-F), and Two-way ANOVA followed by a Bonferroni's multiple comparison (D-F).

Figure 3: Leptin antagonism ameliorates the general health and lifespan of symptomatic *Mecp2*$^{-/y}$ mice.

A) Box plots of the body weight of P40 WT and *Mecp2*$^{-/y}$ mice. **B**) Body weight change (% of P40) as a function of age in sham-, leptin- and anti-leptin treated *Mecp2*$^{-/y}$ mice. The treatment started at P40 and ended at P50. **C**) Box plot of the body weight change (% of P40) at P50 in sham and treated mice at the indicated genotype and treatment. **D**) Severity score of P40 WT and *Mecp2*$^{-/y}$ mice. mean±SEM. **E**) Plots of the severity score in sham- and anti-leptin treated *Mecp2*$^{-/y}$ mice. Connected points indicate individual mice recorded the day before the treatment (P40) and at the end of the treatment (P50). Connected squares indicate mean±SEM. **F**) Radar plot of the symptoms scored in sham and anti-leptin treated *Mecp2*$^{-/y}$ mice. **G**) Plot of the percentage of surviving mice as a function of age. The treatment started at P40 and was maintained until the death of the animal. Numbers in parenthesis indicate the number of mice used. $^{*}P < 0.05$; $^{**}P < 0.01$; $^{***}P < 0.001$, Two-way ANOVA followed by a Bonferroni's multiple comparison (C), two-tailed unpaired *t*-test (A, C,), two-tailed paired *t*-test (D, E).

Figure 4: Leptin antagonism prevents the worsening of locomotor deficit but does not improve motor coordination nor anxiety alterations of symptomatic *Mecp2*$^{-/y}$ mice.

A) Box plots of the distance traveled by P40 WT and *Mecp2*$^{-/y}$ mice in an open field. **B**) Plots of distance traveled by sham and anti-leptin *Mecp2*$^{-/y}$ mice in an open field. Connected points indicate individual mice recorded the day before the treatment (P40) and at the end of the treatment (P50). Connected squares indicate mean±SEM. **C**) Box plots of the distance traveled in an open field by P50 sham and treated mice at the indicated genotype and treatment. **D**) Mean ± SEM plots of the latency to fall (best performance of 3 trials) of P40 WT and *Mecp2*$^{-/y}$ mice in the accelerating rotarod. **E**) Plots of latency to fall (best performance) by sham and anti-leptin *Mecp2*$^{-/y}$ mice. Connected points indicate individual mice recorded the day before the treatment (P40) and at the end of the treatment (P50). Connected squares indicate mean±SEM. **F**) Box plots of the latency to fall (best performance) by P50 sham and treated mice at the indicated genotype and treatment. **G, H**) Box plots of the time spent in open arms (**G**) and dipping (**H**) by P40 WT and *Mecp2*$^{-/y}$ mice, and P50 WT- and *Mecp2*$^{-/y}$-sham and treated mice in an elevated plus maze. mean±SEM. **P* < 0.05; ***P* < 0.01; ****P* < 0.001, two-tailed unpaired *t*-test (A), two-tailed paired *t*-test (B), Wilcoxon matched pairs rank test (E), Mann Whitney test (D), Two-way ANOVA followed by a Bonferroni's multiple comparison (C, F, G, H).

Figure 5: Leptin antagonism during the symptomatic stage does not improve seizure susceptibility of *Mecp2*$^{-/y}$ mice.

A, B) Box plots of tonic-clonic seizures onset latency of P50 untreated (**A**) and treated (**B**) WT and *Mecp2*$^{-/y}$ mice. **C, D**) Flurothyl-induced lethality of P50 untreated (**C**) and treated (**D**) WT and *Mecp2*$^{-/y}$ mice. Numbers in parenthesis indicate the number of mice used. **P<0.05, ****P* < 0.001, Two-tailed unpaired *t*-test (**A, B**), Fisher exact test (**C**).

Figure 6: Leptin contributes to the E/I imbalance in the hippocampus of symptomatic *Mecp2*$^{-/y}$ mice.

A) Examples of whole-cell recordings performed on CA3 pyramidal neurons at a holding potential of −45 and -70 mV at P50. The glutamatergic synaptic currents are inwards and the GABAergic synaptic currents are outwards. **B-D)** Box plots of the ratio of spontaneous glutamatergic and GABAergic postsynaptic currents (**B, C**) and frequency of spontaneous GABAergic postsynaptic currents (**D, E**) recorded from P50 untreated- (**B, D**) and treated- (**C, E**) WT and *Mecp2*$^{-/y}$ CA3 pyramidal neurons. Scale bars: 100pA, 2 sec. Numbers in parenthesis indicate the number of cells recorded and mice used. ***P* < 0.01; ****P* < 0.001, Two-tailed Mann-Whitney test (**B, D**). Two-tailed Kruskal-Wallis test followed by Dunn's post hoc comparison (**C, E**).

Figure 7: Leptin contributes to hippocampal synaptic plasticity impairment of symptomatic *Mecp2*$^{-/y}$ mice.

LTP was recorded for 50 min following two trains of 100 Hz tetanic stimulation (1sec duration, 20 sec interval) at the Schaffer collateral-CA1 synapses of acute hippocampal slices from symptomatic (P50) untreated and treated *Mecp2*$^{-/y}$ and WT mice. Insets show examples of fEPSP. Scale bar: 100µV, 3ms. Numbers in parenthesis indicate the number of slices recorded and mice used. *$P < 0.05$, Repeated measure ANOVA.

Figure 8: RTT-associated symptoms are improved in leptin haplo insufficient mice.

A) Serum leptin levels in P50 WT, *Mecp2*$^{-/y}$ and *Mecp2*$^{-/y;ob/+}$ littermates. **B,C**) Box plots of the frequency ratio of spontaneous glutamatergic and GABAergic postsynaptic currents (B) and frequency of spontaneous GABAergic postsynaptic currents (C) recorded from CA3 pyramidal neurons at P50. **D**) LTP at the Schaffer collateral-CA1 synapses of acute hippocampal slices from symptomatic (P50-60) *Mecp2*$^{-/y}$ and *Mecp2*$^{-/y;ob/+}$ mice. **E,F**) Box plots of apnea frequency (E) and body weight (F) in P50 WT, *Mecp2*$^{-/y}$ and *Mecp2*$^{-/y;ob/+}$ littermates. Numbers in parenthesis indicate the number of mice used and number of cells recorded. *$P < 0.05$; **$P < 0.01$; ***$P < 0.001$. Two-way ANOVA followed by a Bonferroni's multiple comparison (A, D, E), two-tailed Kruskal-Wallis followed by a Dunn's multiple comparison (B,C), repeated measure ANOVA (F).

REFERENCES

Acampa, M., Guideri, F., Hayek, J., Blardi, P., De Lalla, A., Zappella, M., et al. (2008). Sympathetic overactivity and plasma leptin levels in Rett syndrome. *Neurosci. Lett.* 432, 69–72. doi: 10.1016/j.neulet.2007.12.030.

Ahima, R. S., and Flier, J. S. (2000). Leptin. *Annual Review of Physiology* 62, 413–437. doi: 10.1146/annurev.physiol.62.1.413.

Asaka, Y., Jugloff, D. G. M., Zhang, L., Eubanks, J. H., and Fitzsimonds, R. M. (2006). Hippocampal synaptic plasticity is impaired in the Mecp2-null mouse model of Rett syndrome. *Neurobiol Dis* 21, 217–227. doi: 10.1016/j.nbd.2005.07.005.

Ashwood, P., Kwong, C., Hansen, R., Hertz-Picciotto, I., Croen, L., Krakowiak, P., et al. (2008). Brief report: plasma leptin levels are elevated in autism: association with early onset phenotype? *J Autism Dev Disord* 38, 169–175. doi: 10.1007/s10803-006-0353-1.

Bassi, M., Furuya, W. I., Menani, J. V., Colombari, D. S. A., do Carmo, J. M., da Silva, A. A., et al. (2014). Leptin into the ventrolateral medulla facilitates chemorespiratory response in leptin-deficient (ob/ob) mice. *Acta Physiol (Oxf)* 211, 240–248. doi: 10.1111/apha.12257.

Bassi, M., Nakamura, N. B., Furuya, W. I., Colombari, D. S. A., Menani, J. V., do Carmo, J. M., et al. (2015). Activation of the brain melanocortin system is required for leptin-induced modulation of chemorespiratory function. *Acta Physiol (Oxf)* 213, 893–901. doi: 10.1111/apha.12394.

Belcastro, V., D'Egidio, C., Striano, P., and Verrotti, A. (2013). Metabolic and endocrine effects of valproic acid chronic treatment. *Epilepsy Res* 107, 1–8. doi: 10.1016/j.eplepsyres.2013.08.016.

Bertoni, A., Schaller, F., Tyzio, R., Gaillard, S., Santini, F., Xolin, M., et al. (2021). Oxytocin administration in neonates shapes hippocampal circuitry and restores social behavior in a mouse model of autism. *Mol Psychiatry*. doi: 10.1038/s41380-021-01227-6.

Blardi, P., de Lalla, A., Ceccatelli, L., Vanessa, G., Auteri, A., and Hayek, J. (2010). Variations of plasma leptin and adiponectin levels in autistic patients. *Neurosci. Lett.* 479, 54–57. doi: 10.1016/j.neulet.2010.05.027.

Blardi, P., de Lalla, A., D'Ambrogio, T., Vonella, G., Ceccatelli, L., Auteri, A., et al. (2009). Long-term plasma levels of leptin and adiponectin in Rett syndrome. *Clin. Endocrinol. (Oxf)* 70, 706–709. doi: 10.1111/j.1365-2265.2008.03386.x.

Blardi, P., de Lalla, A., D'Ambrogio, T., Zappella, M., Cevenini, G., Ceccatelli, L., et al. (2007). Rett syndrome and plasma leptin levels. *J Pediatr* 150, 37–39. doi: 10.1016/j.jpeds.2006.10.061.

Bouret, S. G., Draper, S. J., and Simerly, R. B. (2004). Trophic action of leptin on hypothalamic neurons that regulate feeding. *Science* 304, 108–110. doi: 10.1126/science.1095004.

Calfa, G., Li, W., Rutherford, J. M., and Pozzo-Miller, L. (2015). Excitation/inhibition imbalance and impaired synaptic inhibition in hippocampal area CA3 of Mecp2 knockout mice. *Hippocampus* 25, 159–168. doi: 10.1002/hipo.22360.

796 Caron, E., Sachot, C., Prevot, V., and Bouret, S. G. (2010). Distribution of leptin-sensitive cells in the
797 postnatal and adult mouse brain. *J. Comp. Neurol.* 518, 459–476. doi: 10.1002/cne.22219.

798 Chahrour, M., and Zoghbi, H. Y. (2007). The story of Rett syndrome: from clinic to neurobiology. *Neuron*
799 56, 422–437. doi: 10.1016/j.neuron.2007.10.001.

800 Chapnik, N., Solomon, G., Genzer, Y., Miskin, R., Gertler, A., and Froy, O. (2013). A superactive leptin
801 antagonist alters metabolism and locomotion in high-leptin mice. *J Endocrinol* 217, 283–290. doi:
802 10.1530/JOE-13-0033.

803 Chen, C.-Y., Di Lucente, J., Lin, Y.-C., Lien, C.-C., Rogawski, M. A., Maezawa, I., et al. (2018).
804 Defective GABAergic neurotransmission in the nucleus tractus solitarius in Mecp2-null mice, a model of
805 Rett syndrome. *Neurobiol Dis* 109, 25–32. doi: 10.1016/j.nbd.2017.09.006.

806 Cheval, H., Guy, J., Merusi, C., De Sousa, D., Selfridge, J., and Bird, A. (2012). Postnatal inactivation
807 reveals enhanced requirement for MeCP2 at distinct age windows. *Hum Mol Genet* 21, 3806–3814. doi:
808 10.1093/hmg/dds208.

809 Conti, V., Gandaglia, A., Galli, F., Tirone, M., Bellini, E., Campana, L., et al. (2015). MeCP2 Affects
810 Skeletal Muscle Growth and Morphology through Non Cell-Autonomous Mechanisms. *PLoS One* 10,
811 e0130183. doi: 10.1371/journal.pone.0130183.

812 Cortelazzo, A., De Felice, C., Guerranti, R., Signorini, C., Leoncini, S., Pecorelli, A., et al. (2014).
813 Subclinical inflammatory status in Rett syndrome. *Mediators Inflamm* 2014, 480980. doi:
814 10.1155/2014/480980.

815 Davis, J. F., Choi, D. L., and Benoit, S. C. (2010). Insulin, leptin and reward. *Trends Endocrinol Metab*
816 21, 68–74. doi: 10.1016/j.tem.2009.08.004.

817 D'Cruz, J. A., Wu, C., Zahid, T., El-Hayek, Y., Zhang, L., and Eubanks, J. H. (2010). Alterations of
818 cortical and hippocampal EEG activity in MeCP2-deficient mice. *Neurobiol Dis* 38, 8–16. doi:
819 10.1016/j.nbd.2009.12.018.

820 Dhar, M., Wayman, G. A., Zhu, M., Lambert, T. J., Davare, M. A., and Appleyard, S. M. (2014). Leptin-
821 induced spine formation requires TrpC channels and the CaM kinase cascade in the hippocampus. *J.*
822 *Neurosci.* 34, 10022–10033. doi: 10.1523/JNEUROSCI.2868-13.2014.

823 Dumon, C., Diabira, D., Chudotvorova, I., Bader, F., Sahin, S., Zhang, J., et al. (2018). The adipocyte
824 hormone leptin sets the emergence of hippocampal inhibition in mice. *Elife* 7, e36726. doi:
825 10.7554/eLife.36726.

826 Ehinger, Y., Matagne, V., Villard, L., and Roux, J.-C. (2018). Rett syndrome from bench to bedside:
827 recent advances. *F1000Res* 7, 398. doi: 10.12688/f1000research.14056.1.

828 Elinav, E., Niv-Spector, L., Katz, M., Price, T. O., Ali, M., Yacobovitz, M., et al. (2009). Pegylated leptin
829 antagonist is a potent orexigenic agent: preparation and mechanism of activity. *Endocrinology* 150, 3083–
830 3091. doi: 10.1210/en.2008-1706.

831 Farr, O. M., Tsoukas, M. A., and Mantzoros, C. S. (2015). Leptin and the brain: influences on brain
832 development, cognitive functioning and psychiatric disorders. *Metabolism* 64, 114–130. doi:
833 10.1016/j.metabol.2014.07.004.

834 Fisch, S., Bachner-Hinenzon, N., Ertracht, O., Guo, L., Arad, Y., Ben-Zvi, D., et al. (2020). Localized
835 Antileptin Therapy Prevents Aortic Root Dilatation and Preserves Left Ventricular Systolic Function in a
836 Murine Model of Marfan Syndrome. *J Am Heart Assoc* 9, e014761. doi: 10.1161/JAHA.119.014761.

837 Fukuhara, S., Nakajima, H., Sugimoto, S., Kodo, K., Shigehara, K., Morimoto, H., et al. (2019). High-fat
838 diet accelerates extreme obesity with hyperphagia in female heterozygous Mecp2-null mice. *PLoS One* 14,
839 e0210184. doi: 10.1371/journal.pone.0210184.

840 Gauda, E. B., Conde, S., Bassi, M., Zoccal, D. B., Almeida Colombari, D. S., Colombari, E., et al. (2020).
841 Leptin: Master Regulator of Biological Functions that Affects Breathing. *Compr Physiol* 10, 1047–1083.
842 doi: 10.1002/cphy.c190031.

843 Gertler, A., and Elinav, E. (2014). Novel superactive leptin antagonists and their potential therapeutic
844 applications. *Curr Pharm Des* 20, 659–665. doi: 10.2174/13816128113199990014.

845 Glaze, D. G. (2002). Neurophysiology of Rett syndrome. *Mental Retardation and Developmental*
846 *Disabilities Research Reviews* 8, 66–71. doi: 10.1002/mrdd.10024.

847 Gonzalez, A., Cheung, W. W., Perens, E. A., Oliveira, E. A., Gertler, A., and Mak, R. H. (2021). A Leptin
848 Receptor Antagonist Attenuates Adipose Tissue Browning and Muscle Wasting in Infantile Nephropathic
849 Cystinosis-Associated Cachexia. *Cells* 10, 1954. doi: 10.3390/cells10081954.

850 Greco, S. J., Bryan, K. J., Sarkar, S., Zhu, X., Smith, M. A., Ashford, J. W., et al. (2010). Leptin reduces
851 pathology and improves memory in a transgenic mouse model of Alzheimer's disease. *J Alzheimers Dis*
852 19, 1155–1167. doi: 10.3233/JAD-2010-1308.

853 Grillo, C. A., Piroli, G. G., Evans, A. N., Macht, V. A., Wilson, S. P., Scott, K. A., et al. (2011).
854 Obesity/hyperleptinemic phenotype adversely affects hippocampal plasticity: effects of dietary restriction.
855 *Physiol Behav* 104, 235–241. doi: 10.1016/j.physbeh.2010.10.020.

856 Guimond, D., Diabira, D., Porcher, C., Bader, F., Ferrand, N., Zhu, M., et al. (2014). Leptin potentiates
857 GABAergic synaptic transmission in the developing rodent hippocampus. *Frontiers in Cellular*
858 *Neuroscience* 8, 235. doi: 10.3389/fncel.2014.00235.

859 Guo, M., Huang, T.-Y., Garza, J. C., Chua, S. C., and Lu, X.-Y. (2013). Selective deletion of leptin
860 receptors in adult hippocampus induces depression-related behaviours. *Int. J. Neuropsychopharmacol.* 16,
861 857–867. doi: 10.1017/S1461145712000703.

862 Guo, M., Lu, Y., Garza, J. C., Li, Y., Chua, S. C., Zhang, W., et al. (2012). Forebrain glutamatergic
863 neurons mediate leptin action on depression-like behaviors and synaptic depression. *Transl Psychiatry* 2,
864 e83. doi: 10.1038/tp.2012.9.

865 Guy, J., Gan, J., Selfridge, J., Cobb, S., and Bird, A. (2007). Reversal of neurological defects in a mouse
866 model of Rett syndrome. *Science* 315, 1143–1147. doi: 10.1126/science.1138389.

867 Guy, J., Hendrich, B., Holmes, M., Martin, J. E., and Bird, A. (2001). A mouse Mecp2-null mutation
868 causes neurological symptoms that mimic Rett syndrome. *Nat Genet* 27, 322–326. doi: 10.1038/85899.

869 Harvey, J. (2003). Leptin: a multifaceted hormone in the central nervous system. *Mol Neurobiol* 28, 245–
870 258. doi: 10.1385/MN:28:3:245.

871 Harvey, J. (2022). Food for Thought: Leptin and Hippocampal Synaptic Function. *Front Pharmacol* 13,
872 882158. doi: 10.3389/fphar.2022.882158.

873 Harvey, J., Solovyova, N., and Irving, A. (2006). Leptin and its role in hippocampal synaptic plasticity.
874 *Prog Lipid Res* 45, 369–378. doi: 10.1016/j.plipres.2006.03.001.

875 Inyushkin, A. N., Inyushkina, E. M., and Merkulova, N. A. (2009). Respiratory responses to
876 microinjections of leptin into the solitary tract nucleus. *Neurosci Behav Physiol* 39, 231–240. doi:
877 10.1007/s11055-009-9124-8.

878 Katz, D. M., Dutschmann, M., Ramirez, J.-M., and Hilaire, G. (2009). Breathing disorders in Rett
879 syndrome: progressive neurochemical dysfunction in the respiratory network after birth. *Respir Physiol*
880 *Neurobiol* 168, 101–108. doi: 10.1016/j.resp.2009.04.017.

881 Kerr, B., Silva, P. A., Walz, K., and Young, J. I. (2010). Unconventional Transcriptional Response to
882 Environmental Enrichment in a Mouse Model of Rett Syndrome. *PLOS ONE* 5, e11534. doi:
883 10.1371/journal.pone.0011534.

884 Lewis, J. D., Meehan, R. R., Henzel, W. J., Maurer-Fogy, I., Jeppesen, P., Klein, F., et al. (1992).
885 Purification, sequence, and cellular localization of a novel chromosomal protein that binds to methylated
886 DNA. *Cell* 69, 905–914. doi: 10.1016/0092-8674(92)90610-o.

887 Li, L.-L., Jin, M.-F., and Ni, H. (2018). Zinc/CaMK II Associated-Mitophagy Signaling Contributed to
888 Hippocampal Mossy Fiber Sprouting and Cognitive Deficits Following Neonatal Seizures and Its
889 Regulation by Chronic Leptin Treatment. *Front Neurol* 9, 802. doi: 10.3389/fneur.2018.00802.

890 Li, W. (2022). Excitation and Inhibition Imbalance in Rett Syndrome. *Front Neurosci* 16, 825063. doi:
891 10.3389/fnins.2022.825063.

892 Lim, G., Wang, S., Zhang, Y., Tian, Y., and Mao, J. (2009). Spinal leptin contributes to the pathogenesis
893 of neuropathic pain in rodents. *J Clin Invest* 119, 295–304. doi: 10.1172/JCI36785.

894 Liu, C., Wang, J., Wei, Y., Zhang, W., Geng, M., Yuan, Y., et al. (2019). Fat-Specific Knockout of Mecp2
895 Upregulates Slpi to Reduce Obesity by Enhancing Browning. *Diabetes* 69, 35–47. doi: 10.2337/db19-
896 0502.

897 Lozovaya, N., Nardou, R., Tyzio, R., Chiesa, M., Pons-Bennaceur, A., Eftekhari, S., et al. (2019). Early
898 alterations in a mouse model of Rett syndrome: the GABA developmental shift is abolished at birth. *Sci*
899 *Rep* 9, 9276. doi: 10.1038/s41598-019-45635-9.

900 McGregor, G., and Harvey, J. (2019). Leptin Regulation of Synaptic Function at Hippocampal TA-CA1
901 and SC-CA1 Synapses: Implications for Health and Disease. *Neurochem Res* 44, 650–660. doi:
902 10.1007/s11064-017-2362-1.

903 Medrihan, L., Tantalaki, E., Aramuni, G., Sargsyan, V., Dudanova, I., Missler, M., et al. (2008). Early
904 defects of GABAergic synapses in the brain stem of a MeCP2 mouse model of Rett syndrome. *J*
905 *Neurophysiol* 99, 112–121. doi: 10.1152/jn.00826.2007.

906 Mora-Muñoz, L., Guerrero-Naranjo, A., Rodríguez-Jimenez, E. A., Mastronardi, C. A., and Velez-van-
907 Meerbeke, A. (2018). Leptin: role over central nervous system in epilepsy. *BMC Neurosci* 19, 51. doi:
908 10.1186/s12868-018-0453-9.

909 Moretti, P., Levenson, J. M., Battaglia, F., Atkinson, R., Teague, R., Antalffy, B., et al. (2006). Learning
910 and memory and synaptic plasticity are impaired in a mouse model of Rett syndrome. *J Neurosci* 26, 319–
911 327. doi: 10.1523/JNEUROSCI.2623-05.2006.

912 Motil, K. J., Barrish, J. O., Lane, J., Geerts, S. P., Annese, F., McNair, L., et al. (2011). Vitamin D
913 deficiency is prevalent in girls and women with Rett syndrome. *J Pediatr Gastroenterol Nutr* 53, 569–
914 574. doi: 10.1097/MPG.0b013e3182267a66.

915 Moult, P. R., and Harvey, J. (2008). Hormonal regulation of hippocampal dendritic morphology and
916 synaptic plasticity. *Cell Adh Migr* 2, 269–275. doi: 10.4161/cam.2.4.6354.

917 Moult, P. R., and Harvey, J. (2009). Regulation of glutamate receptor trafficking by leptin. *Biochem Soc*
918 *Trans* 37, 1364–1368. doi: 10.1042/BST0371364.

919 Neyens, D., Zhao, H., Huston, N. J., Wayman, G. A., Ritter, R. C., and Appleyard, S. M. (2020). Leptin
920 Sensitizes NTS Neurons to Vagal Input by Increasing Postsynaptic NMDA Receptor Currents. *J Neurosci*
921 40, 7054–7064. doi: 10.1523/JNEUROSCI.1865-19.2020.

922 O'Malley, D., MacDonald, N., Mizielinska, S., Connolly, C. N., Irving, A. J., and Harvey, J. (2007).
923 Leptin promotes rapid dynamic changes in hippocampal dendritic morphology. *Mol Cell Neurosci* 35,
924 559–572. doi: 10.1016/j.mcn.2007.05.001.

925 Oomura, Y., Hori, N., Shiraishi, T., Fukunaga, K., Takeda, H., Tsuji, M., et al. (2006). Leptin facilitates
926 learning and memory performance and enhances hippocampal CA1 long-term potentiation and CaMK II
927 phosphorylation in rats. *Peptides* 27, 2738–2749. doi: 10.1016/j.peptides.2006.07.001.

928 Park, M. J., Aja, S., Li, Q., Degano, A. L., Penati, J., Zhuo, J., et al. (2014). Anaplerotic triheptanoin diet
929 enhances mitochondrial substrate use to remodel the metabolome and improve lifespan, motor function,
930 and sociability in MeCP2-null mice. *PLoS One* 9, e109527. doi: 10.1371/journal.pone.0109527.

931 Pinto, S., Roseberry, A. G., Liu, H., Diano, S., Shanabrough, M., Cai, X., et al. (2004). Rapid rewiring of
932 arcuate nucleus feeding circuits by leptin. *Science* 304, 110–115. doi: 10.1126/science.1089459.

933 Raghavan, R., Zuckerman, B., Hong, X., Wang, G., Ji, Y., Paige, D., et al. (2018). Fetal and Infancy
934 Growth Pattern, Cord and Early Childhood Plasma Leptin, and Development of Autism Spectrum
935 Disorder in the Boston Birth Cohort. *Autism Res* 11, 1416–1431. doi: 10.1002/aur.2011.

936 Ramirez, J.-M., Ward, C. S., and Neul, J. L. (2013). Breathing challenges in Rett syndrome: lessons
937 learned from humans and animal models. *Respir Physiol Neurobiol* 189, 280–287. doi:
938 10.1016/j.resp.2013.06.022.

939 Ricceri, L., De Filippis, B., and Laviola, G. (2008). Mouse models of Rett syndrome: from behavioural
940 phenotyping to preclinical evaluation of new therapeutic approaches. *Behav Pharmacol* 19, 501–517. doi:
941 10.1097/FBP.0b013e32830c3645.

942 Sahin, G. S., Dhar, M., Dillon, C., Zhu, M., Shiina, H., Winters, B. D., et al. (2020). Leptin stimulates
943 synaptogenesis in hippocampal neurons via KLF4 and SOCS3 inhibition of STAT3 signaling. *Mol Cell*
944 *Neurosci* 106, 103500. doi: 10.1016/j.mcn.2020.103500.

945 Sahin, G. S., Luis Rodriguez-Llamas, J., Dillon, C., Medina, I., Appleyard, S. M., Gaiarsa, J.-L., et al.
946 (2021). Leptin increases GABAergic synaptogenesis through the Rho guanine exchange factor β-PIX in
947 developing hippocampal neurons. *Sci Signal* 14, eabe4111. doi: 10.1126/scisignal.abe4111.

948 Sandweiss, A. J., Brandt, V. L., and Zoghbi, H. Y. (2020). Advances in understanding of Rett syndrome
949 and MECP2 duplication syndrome: prospects for future therapies. *Lancet Neurol* 19, 689–698. doi:
950 10.1016/S1474-4422(20)30217-9.

951 Scaramuzza, L., De Rocco, G., Desiato, G., Cobolli Gigli, C., Chiacchiaretta, M., Mirabella, F., et al.
952 (2021). The enhancement of activity rescues the establishment of Mecp2 null neuronal phenotypes. *EMBO*
953 *Mol Med*, e12433. doi: 10.15252/emmm.202012433.

954 Sciorati, C., Clementi, E., Manfredi, A. A., and Rovere-Querini, P. (2015). Fat deposition and
955 accumulation in the damaged and inflamed skeletal muscle: cellular and molecular players. *Cell Mol Life*
956 *Sci* 72, 2135–2156. doi: 10.1007/s00018-015-1857-7.

957 Shanley, L. J., Irving, A. J., Rae, M. G., Ashford, M. L. J., and Harvey, J. (2002). Leptin inhibits rat
958 hippocampal neurons via activation of large conductance calcium-activated K+ channels. *Nat Neurosci* 5,
959 299–300. doi: 10.1038/nn824.

960 Signore, A. P., Zhang, F., Weng, Z., Gao, Y., and Chen, J. (2008). Leptin neuroprotection in the CNS:
961 mechanisms and therapeutic potentials. *J. Neurochem.* 106, 1977–1990. doi: 10.1111/j.1471-
962 4159.2008.05457.x.

963 Singh, U. P., Singh, N. P., Guan, H., Busbee, B., Price, R. L., Taub, D. D., et al. (2013). Leptin antagonist
964 ameliorates chronic colitis in IL-$10^{-}/^{-}$ mice. *Immunobiology* 218, 1439–1451. doi:
965 10.1016/j.imbio.2013.04.020.

966 Solovyova, N., Moult, P. R., Milojkovic, B., Lambert, J. J., and Harvey, J. (2009). Bi-directional
967 modulation of fast inhibitory synaptic transmission by leptin. *J. Neurochem.* 108, 190–201. doi:
968 10.1111/j.1471-4159.2008.05751.x.

969 Stagi, S., Cavalli, L., Congiu, L., Scusa, M. F., Ferlini, A., Bigoni, S., et al. (2015). Thyroid function in
970 Rett syndrome. *Horm Res Paediatr* 83, 118–125. doi: 10.1159/000370066.

971 Torres-Andrade, R., Moldenhauer, R., Gutierrez-Bertín, N., Soto-Covasich, J., Mancilla-Medina, C.,
972 Ehrenfeld, C., et al. (2014). The increase in body weight induced by lack of methyl CpG binding protein-2
973 is associated with altered leptin signalling in the hypothalamus. *Exp. Physiol.* 99, 1229–1240. doi:
974 10.1113/expphysiol.2014.079798.

975 Valladolid-Acebes, I., Merino, B., Principato, A., Fole, A., Barbas, C., Lorenzo, M. P., et al. (2012). High-
976 fat diets induce changes in hippocampal glutamate metabolism and neurotransmission. *Am J Physiol*
977 *Endocrinol Metab* 302, E396-402. doi: 10.1152/ajpendo.00343.2011.

978 Vong, L., Ye, C., Yang, Z., Choi, B., Chua, S., and Lowell, B. B. (2011). Leptin action on GABAergic
979 neurons prevents obesity and reduces inhibitory tone to POMC neurons. *Neuron* 71, 142–154. doi:
980 10.1016/j.neuron.2011.05.028.

981 Wang, X., Lacza, Z., Sun, Y. E., and Han, W. (2014). Leptin resistance and obesity in mice with deletion
982 of methyl-CpG-binding protein 2 (MeCP2) in hypothalamic pro-opiomelanocortin (POMC) neurons.
983 *Diabetologia* 57, 236–245. doi: 10.1007/s00125-013-3072-0.

984 Williams, K. W., and Smith, B. N. (2006). Rapid inhibition of neural excitability in the nucleus tractus
985 solitarii by leptin: implications for ingestive behaviour. *J Physiol* 573, 395–412. doi:
986 10.1113/jphysiol.2006.106336.

Yu, H., Shi, L., Chen, J., Jun, S., Hao, Y., Wang, S., et al. (2022). A Neural Circuit Mechanism Controlling Breathing by Leptin in the Nucleus Tractus Solitarii. *Neurosci Bull* 38, 149–165. doi: 10.1007/s12264-021-00742-4.

Zuure, W. A., Roberts, A. L., Quennell, J. H., and Anderson, G. M. (2013). Leptin signaling in GABA neurons, but not glutamate neurons, is required for reproductive function. *J Neurosci* 33, 17874–17883. doi: 10.1523/JNEUROSCI.2278-13.2013.

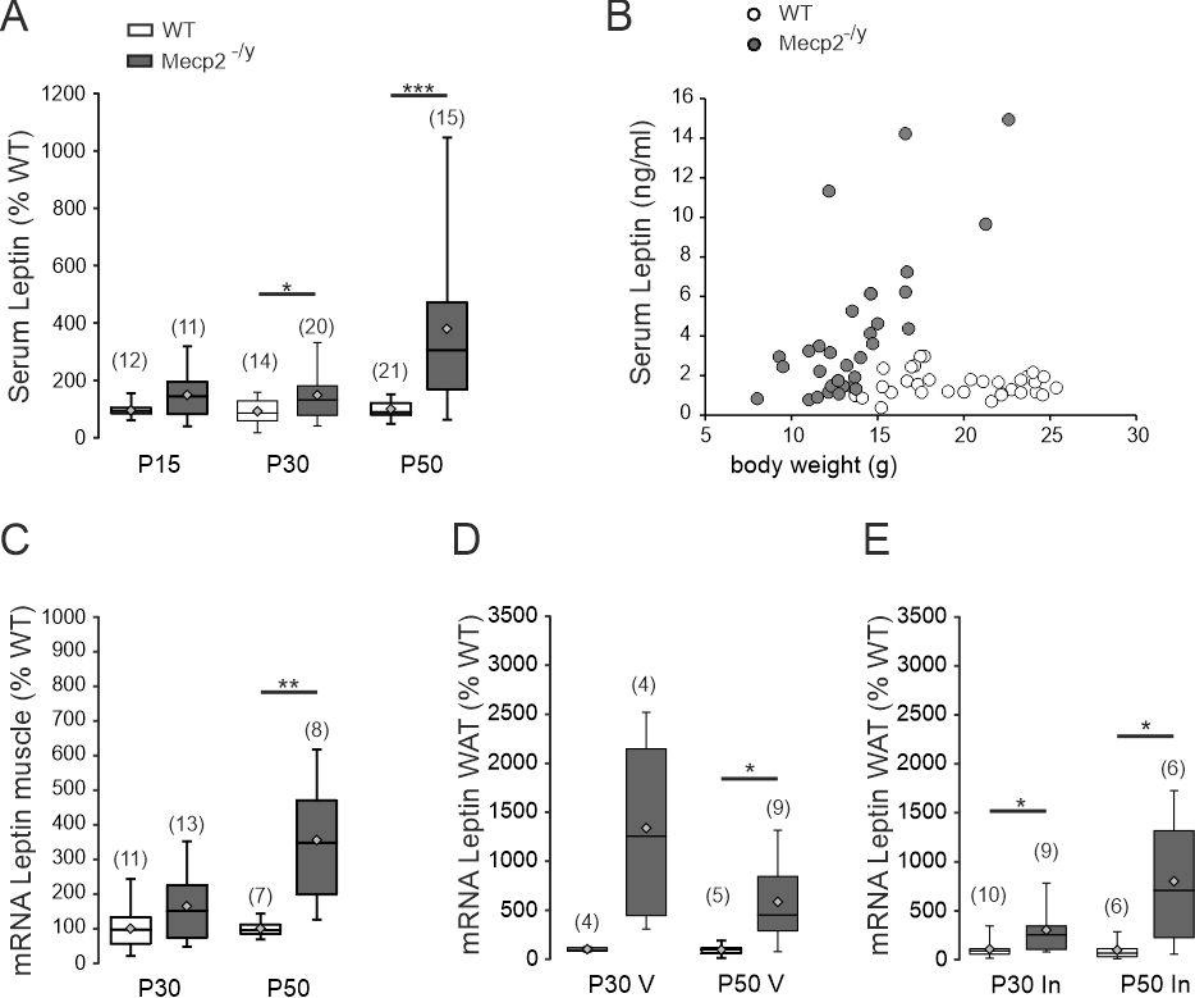
A
WT
Mecp2 -/y
Serum Leptin (% WT)
1200
1000
800
600
400
200
0
***
*
(12)
(11)
(14)
(20)
(21)
(15)
P15
P30
P50
B
WT
Mecp2-/y
Serum Leptin (ng/ml)
16
14
12
10
8
6
4
2
0
5
10
15
20
25
30
body weight (g)
C
mRNA Leptin muscle (% WT)
1000
900
800
700
600
500
400
300
200
100
0
**
(11)
(13)
(7)
(8)
P30
P50
D
mRNA Leptin WAT (% WT)
3500
3000
2500
2000
1500
1000
500
0
(4)
(4)
*
(5)
(9)
P30 V
P50 V
E
mRNA Leptin WAT (% WT)
3500
3000
2500
2000
1500
1000
500
0
*
*
(10)
(9)
(6)
(6)
P30 In
P50 In

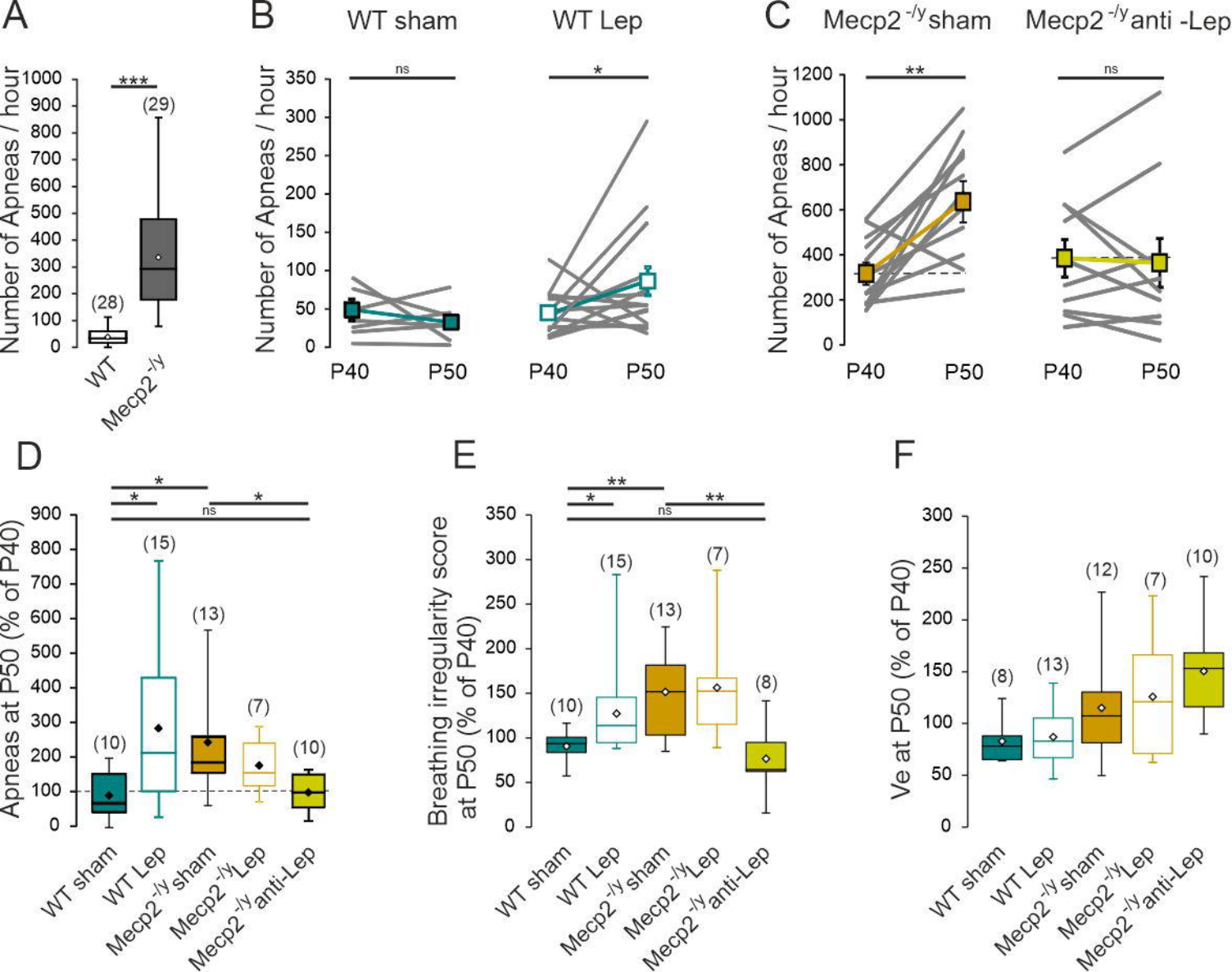
A
B
WT sham
WT Lep
C
Mecp2 -/y sham
Mecp2 -/y anti -Lep
Number of Apneas / hour
***
(28)
(29)
WT
Mecp2 -/y
ns
*
**
P40
P50
D
E
F
Apneas at P50 (% of P40)
Breathing irregularity score at P50 (% of P40)
Ve at P50 (% of P40)
(10)
(15)
(13)
(7)
(8)
(12)
WT sham
WT Lep
Mecp2 -/y sham
Mecp2 -/y Lep
Mecp2 -/y anti-Lep

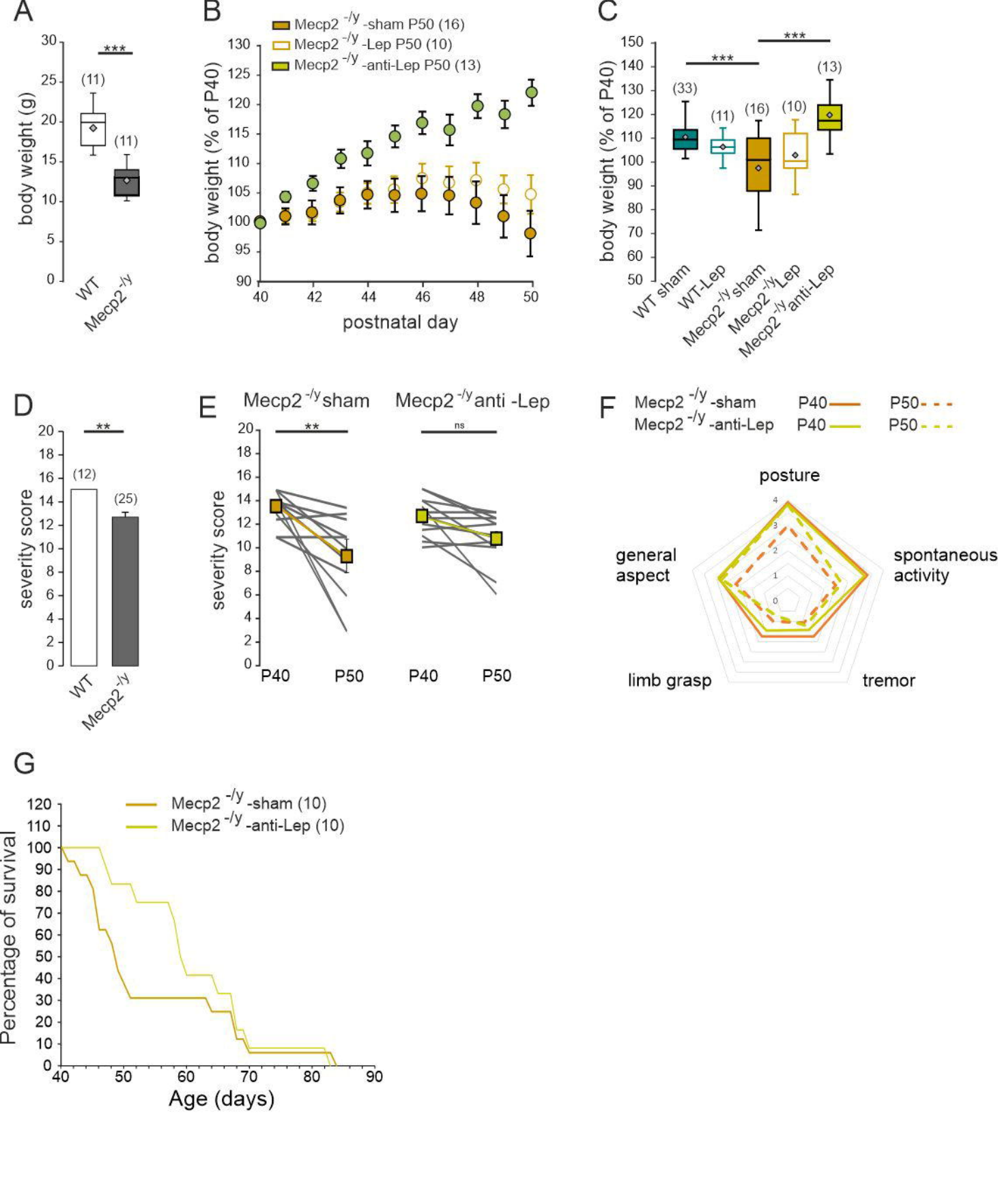
A
body weight (g)
***
(11)
(11)
WT
Mecp2 -/y
B
Mecp2 -/y -sham P50 (16)
Mecp2 -/y -Lep P50 (10)
Mecp2 -/y -anti-Lep P50 (13)
body weight (% of P40)
postnatal day
C
body weight (% of P40)
***
***
(33)
(11)
(16)
(10)
(13)
WT sham
WT-Lep
Mecp2 -/y sham
Mecp2 -/y Lep
Mecp2 -/y anti-Lep
D
severity score
**
(12)
(25)
WT
Mecp2 -/y
E
Mecp2 -/y sham
Mecp2 -/y anti -Lep
severity score
**
ns
P40
P50
P40
P50
F
Mecp2 -/y -sham
Mecp2 -/y -anti-Lep
P40
P50
P40
P50
posture
general aspect
spontaneous activity
limb grasp
tremor
G
Mecp2 -/y -sham (10)
Mecp2 -/y -anti-Lep (10)
Percentage of survival
Age (days)

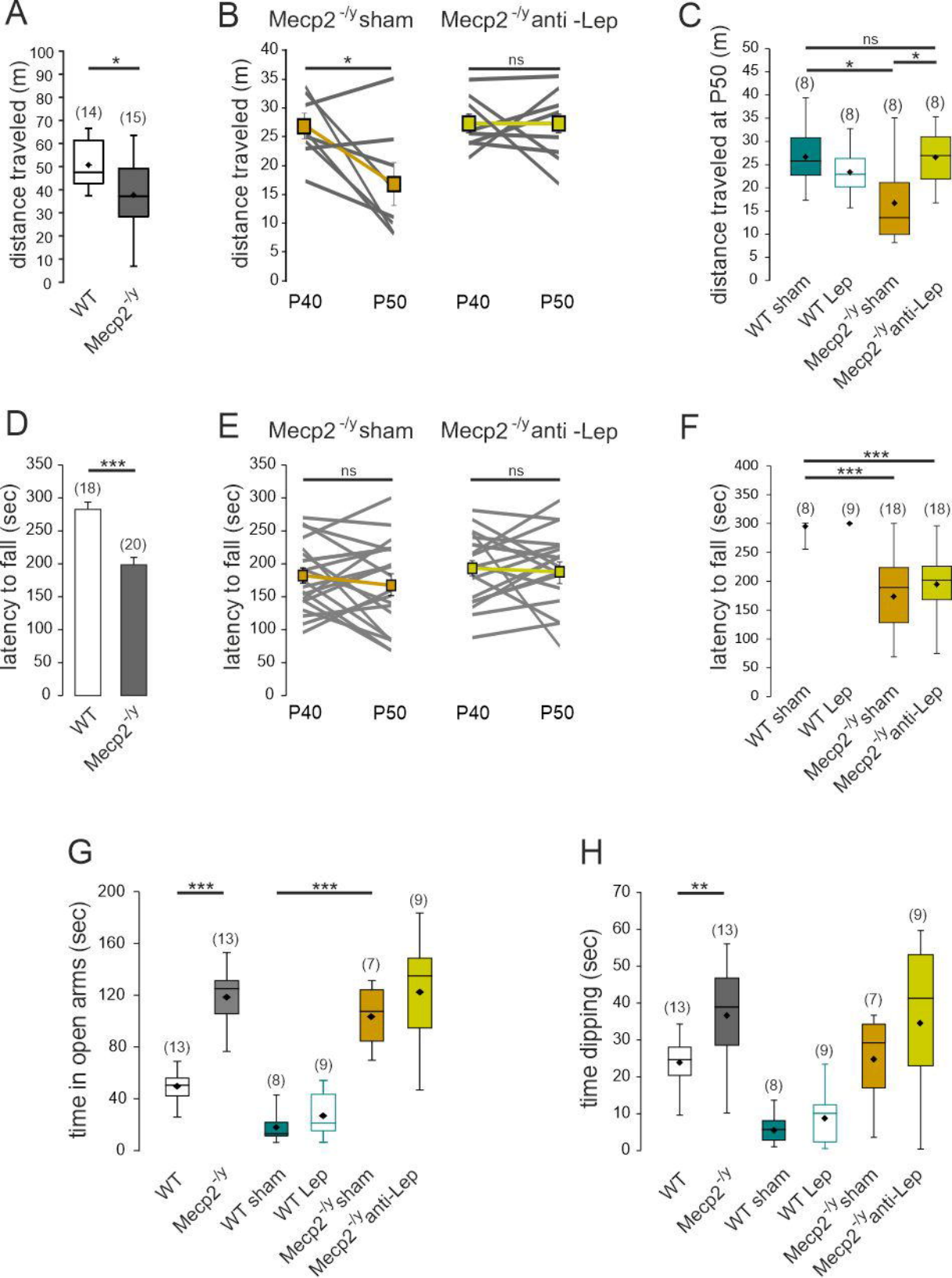
A
distance traveled (m)
*
(14)
(15)
WT
Mecp2 -/y
B
Mecp2 -/y sham
Mecp2 -/y anti -Lep
distance traveled (m)
*
ns
P40
P50
P40
P50
C
distance traveled at P50 (m)
ns
*
*
(8)
(8)
(8)
(8)
WT sham
WT Lep
Mecp2 -/y sham
Mecp2 -/y anti-Lep
D
latency to fall (sec)
***
(18)
(20)
WT
Mecp2 -/y
E
Mecp2 -/y sham
Mecp2 -/y anti -Lep
latency to fall (sec)
ns
ns
P40
P50
P40
P50
F
latency to fall (sec)
***
***
(8)
(9)
(18)
(18)
WT sham
WT Lep
Mecp2 -/y sham
Mecp2 -/y anti-Lep
G
time in open arms (sec)
***
***
(13)
(13)
(8)
(9)
(7)
(9)
WT
Mecp2 -/y
WT sham
WT Lep
Mecp2 -/y sham
Mecp2 -/y anti-Lep
H
time dipping (sec)
**
(13)
(13)
(8)
(9)
(7)
(9)
WT
Mecp2 -/y
WT sham
WT Lep
Mecp2 -/y sham
Mecp2 -/y anti-Lep

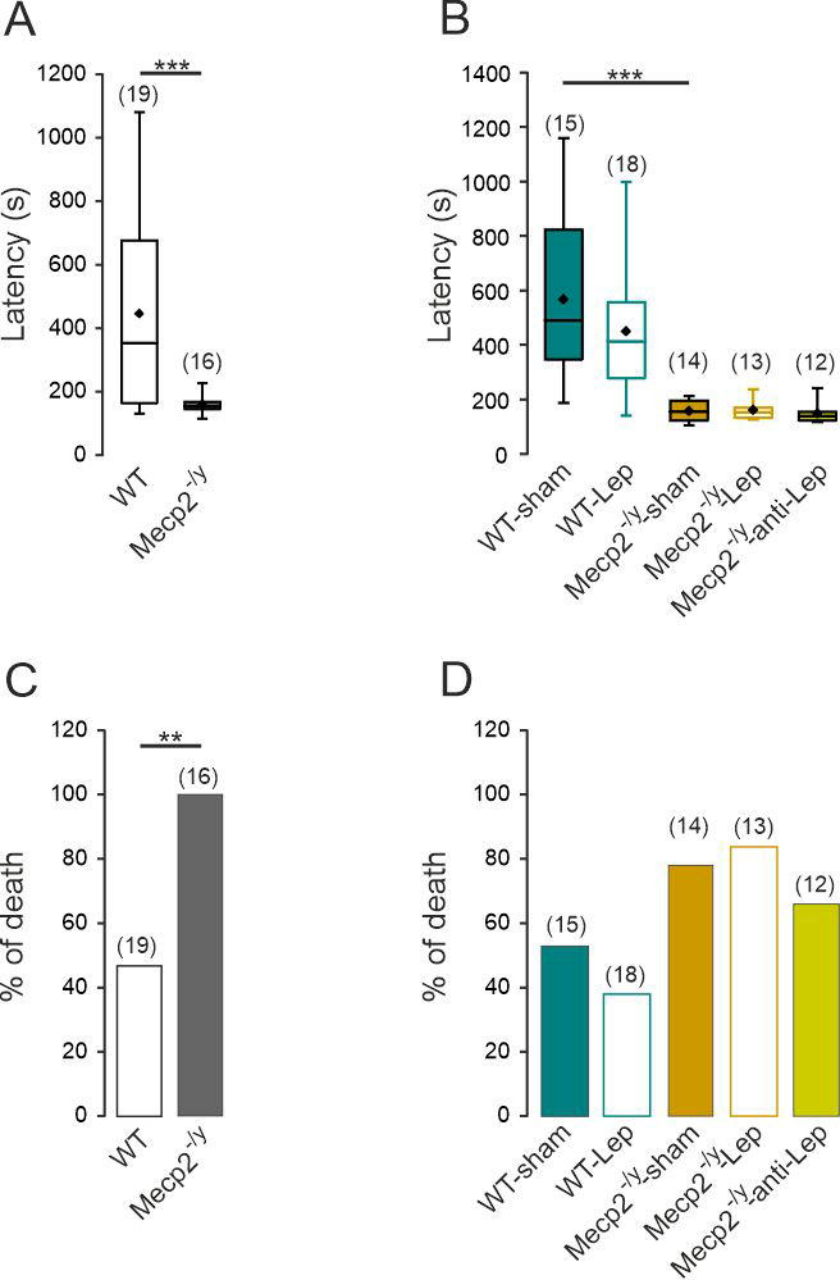
A
B
C
D
Latency (s)
% of death
***
**
(19)
(16)
(15)
(18)
(14)
(13)
(12)
WT
Mecp2 -/y
WT-sham
WT-Lep
Mecp2 -/y sham
Mecp2 -/y Lep
Mecp2 -/y anti-Lep

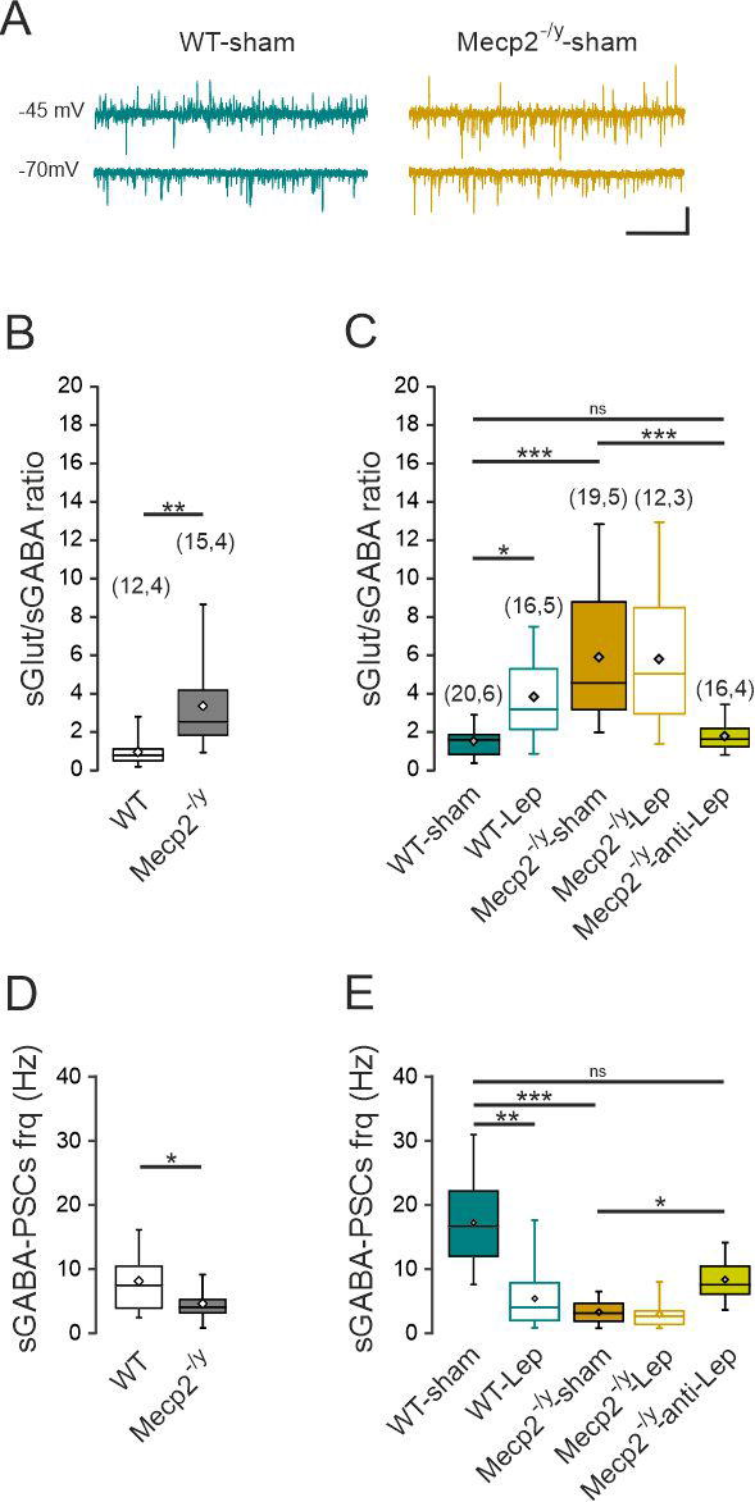
A
WT-sham
Mecp2-/y-sham
-45 mV
-70mV
B
sGlut/sGABA ratio
**
(15,4)
(12,4)
WT
Mecp2 -/y
C
sGlut/sGABA ratio
ns
***
***
*
(19,5)
(12,3)
(16,5)
(20,6)
(16,4)
WT-sham
WT-Lep
Mecp2 -/y-sham
Mecp2 -/y-Lep
Mecp2 -/y-anti-Lep
D
sGABA-PSCs frq (Hz)
*
WT
Mecp2 -/y
E
sGABA-PSCs frq (Hz)
ns
***
**
*
WT-sham
WT-Lep
Mecp2 -/y-sham
Mecp2 -/y-Lep
Mecp2 -/y-anti-Lep

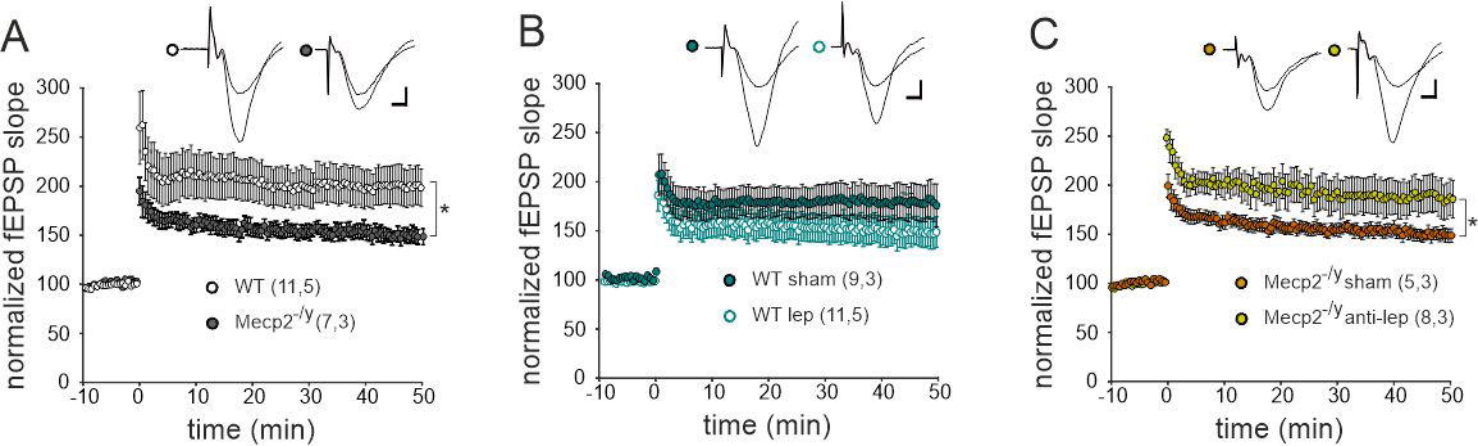
A
normalized fEPSP slope
300
250
200
150
100
50
0
-10
0
10
20
30
40
50
time (min)
WT (11,5)
Mecp2-/y (7,3)
*
B
normalized fEPSP slope
time (min)
WT sham (9,3)
WT lep (11,5)
C
normalized fEPSP slope
time (min)
Mecp2-/y sham (5,3)
Mecp2-/y anti-lep (8,3)
*

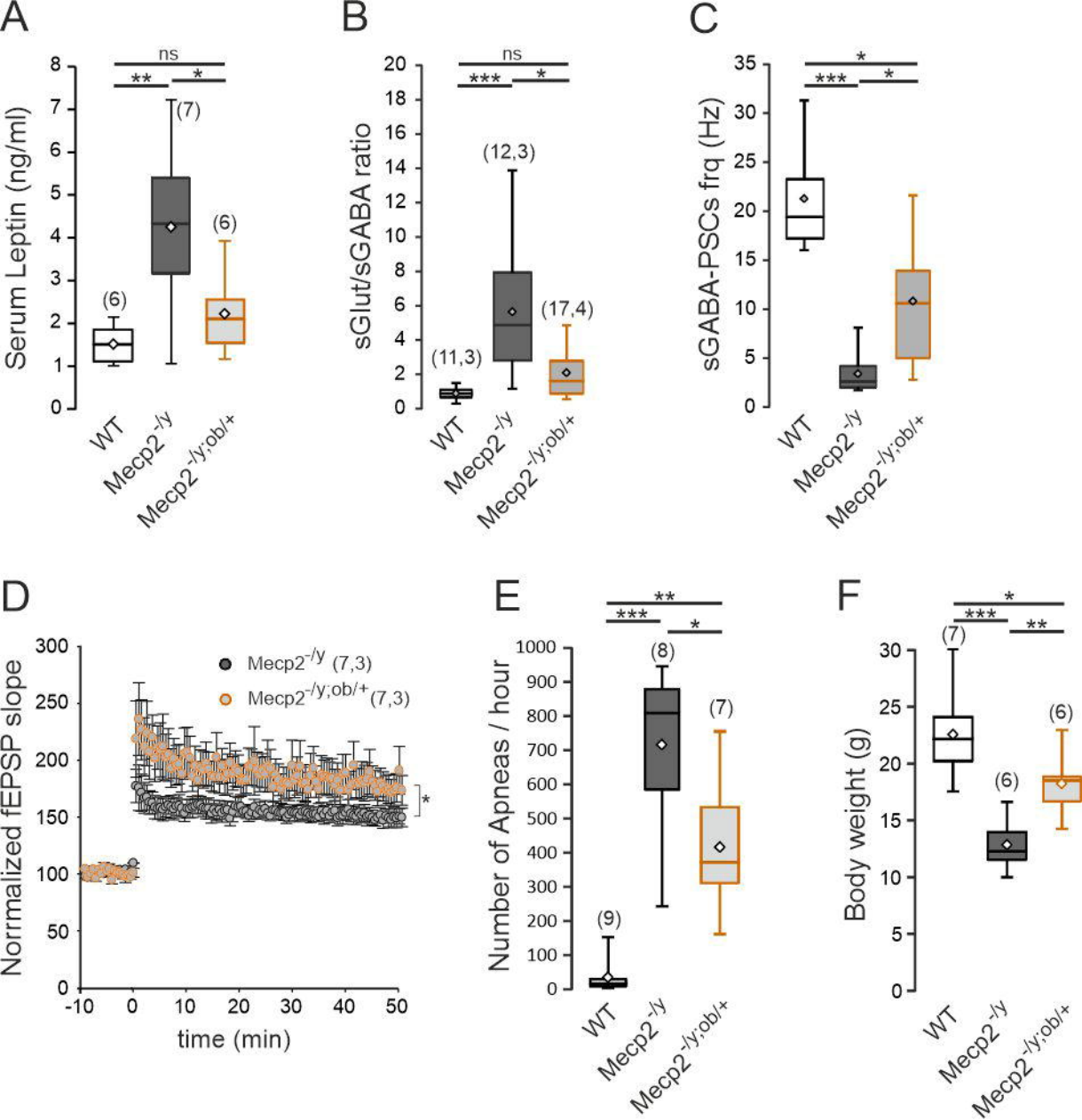
A
Serum Leptin (ng/ml)
ns
**
*
(6)
(7)
(6)
WT
Mecp2-/y
Mecp2-/y;ob/+
B
sGlut/sGABA ratio
ns
***
*
(11,3)
(12,3)
(17,4)
C
sGABA-PSCs frq (Hz)
*
***
*
D
Normalized fEPSP slope
Mecp2-/y (7,3)
Mecp2-/y;ob/+ (7,3)
time (min)
E
Number of Apneas / hour
**
***
*
(9)
(8)
(7)
F
Body weight (g)
*
***
**
(7)
(6)
(6)